Advanced Beam Dynamics in Circular Accelerator and Circular Colliders

Jie Gao

gaoj@ihep.ac.cn

Institute of High Energy Physics, CAS, China

8th International School on Beam Dynamics and Accelerator Technology (ISBA25), Sept. 1-10, 2025, SARI, Shanghai, China

Contents

Introduction

- Storage ring is an important type of accelerators, which is widely used in circular colliders and synchrotron radiation facilities, etc.

- In a storage ring, the most important accelerator physics issue is the dynamic aperture, which limit the ultimate performance of the storage ring, and it is therefore extrememly important to study ,understand, and master this important problem theoretically.

- Beam-beam effects which are special case of nonlinear force effects are the key problems in circular colliders both lepton and hadron ones.

- Single bunch collective effect issues, both in longitudinal and transverse directions, for example, are other limiting factors in storage rings

ELSEVIER
Nuclear Instruments and Methods in Physics Research A 451 (2000) 545–557
NUCLEAR INSTRUMENTS & METHODS IN PHYSICS RESEARCH Section A
www.elsevier.nl/locate/nima

Analytical estimation of the dynamic apertures of circular accelerators

J. Gao*

Laboratoire de L'Accélérateur Linéaire, IN2P3-CNRS et Université de Paris-Sud, B.P. 34, 91898 Orsay cedex, France

Received 28 October 1999; received in revised form 16 February 2000; accepted 26 February 2000

We start with the discussion on dynamic aperture theory in this paper

J. Gao, "Analytical estimation of the dynamic apertures ofcircular accelerators", **Nuclear Instruments and Methods in Physics Research A** 451 (2000) 545-557.

Basic theroy of dynamic aperture

$$H = \frac{p^2}{2} + \frac{K(s)}{2}x^2$$

$$\Psi_1 = \Psi + \frac{2\pi v}{L} - \int_0^s \frac{ds'}{\beta_x(s')}$$

$$J_1 = J$$

$$H_1 = \frac{2\pi v}{L} J_1 .$$

$$x = \sqrt{2J_1\beta_x(s)}\cos\left(\Psi_1 - \frac{2\pi v}{L}s + \int_0^s \frac{ds'}{\beta_x(s')}\right).$$

Linear storage ring

A linear storage ring lattice

$$H = \frac{p^2}{2} + \frac{K(s)}{2}x^2 + \frac{1}{3!B\rho}\frac{\partial^2 B_z}{\partial x^2}x^3 L \sum_{k=-\infty}^{\infty}\delta(s-kL)$$
$$+ \frac{1}{4!B\rho}\frac{\partial^3 B_z}{\partial x^3}x^4 L \sum_{k=-\infty}^{\infty}\delta(s-kL). \qquad (21)$$

$$B_z = B_0(1 + xb_1 + x^2 b_2 + x^3 b_3)$$

$$H = \frac{2\pi v}{L}J_1$$
$$+ \frac{(2J_1\beta_x(s_1))^{3/2}}{3\rho} b_2 L \cos^3\Psi_1 \sum_{k=-\infty}^{\infty}\delta(s-kL)$$
$$+ \frac{(J_1\beta_x(s_2))^2}{\rho} b_3 L \cos^4\Psi_1 \sum_{k=-\infty}^{\infty}\delta(s-kL)$$

Storage ring with nonlinear multipoles

A nonlinear multipole

A storage ring lattice with nonlinear magnetic multipoles

Sextupole term

$$\frac{dJ_1}{ds} = -\frac{\partial H_1}{\partial \Psi_1}$$

$$\frac{d\Psi_1}{ds} = \frac{\partial H_1}{\partial J_1}$$

$$\overline{J_1} = \overline{J_1}(\Psi_1, J_1)$$

$$\overline{\Psi_1} = \overline{\Psi_1}(\Psi_1, J_1)$$

$$\overline{J_1} = J_1 - \frac{(2J_1\beta_x(s_1))^{3/2}}{3\rho} b_2 L \frac{d\cos^3\Psi_1}{d\Psi_1} - \frac{(J_1\beta_x(s_2))^2}{\rho} b_3 L \frac{d\cos^4\Psi_1}{d\Psi_1} \quad (30)$$

$$= \Psi_1 + 2\pi\nu + \frac{\sqrt{2}\beta_x(s_1)^{3/2}\overline{J_1}^{1/2}}{\rho} b_2 L \cos^3\Psi_1 + \frac{2\beta_x(s_2)^2}{\rho}\overline{J_1} b_3 L \cos^4\Psi_1. \quad (31)$$

$$\overline{J_1} = J_1 + A\sin 3\Psi_1$$

$$\overline{\Psi_1} = \Psi_1 + B\overline{J_1}$$

octupole term

$$\overline{J_1} = J_1 + A\sin 4\Psi_1$$

$$\overline{\Psi_1} = \Psi_1 + B\overline{J_1}$$

$$\bar{I} = I + K_0 \sin\theta$$

$$\bar{\theta} = \theta + \bar{I}$$

$$A = \frac{(2J_1\beta_x(s_1))^{3/2}}{4}\left(\frac{b_2 L}{\rho}\right)$$

$$B = \sqrt{2}\beta_x(s_1)^{3/2} J_1^{-1/2}\left(\frac{b_2 L}{\rho}\right)$$

with $\theta = 3\Psi$, $I = 3BJ_1$ and $K_0 = 3AB$. By virtue of the Chirikov criterion [9] it is known that when $|K_0| \geq 0.97164$ [10] resonance overlapping occurs which results in particles' stochastic motions and diffusion processes. Therefore,

$$A_{\mathrm{dyna.sext}} = \sqrt{2J_{\mathrm{max.sext}}\beta_x(s)}$$

$$= \frac{\sqrt{2\beta_x(s)}}{\sqrt{3}\beta_x(s_1)^{3/2}}\left(\frac{\rho}{|b_2|L}\right).$$

$|K_0| \leq 1$ (0.97164) → **Analytical DA expressions**

Standard Map

The progresses of nonlinear physics are the bases for understanding various long stadind beam dynamics phenomenons.

$$\bar{I} = I + K_0 \sin\theta$$

$$\bar{\theta} = \theta + \bar{I}$$

when K≥0.97164 stochastic motion starts, so called Chirikov Criterion

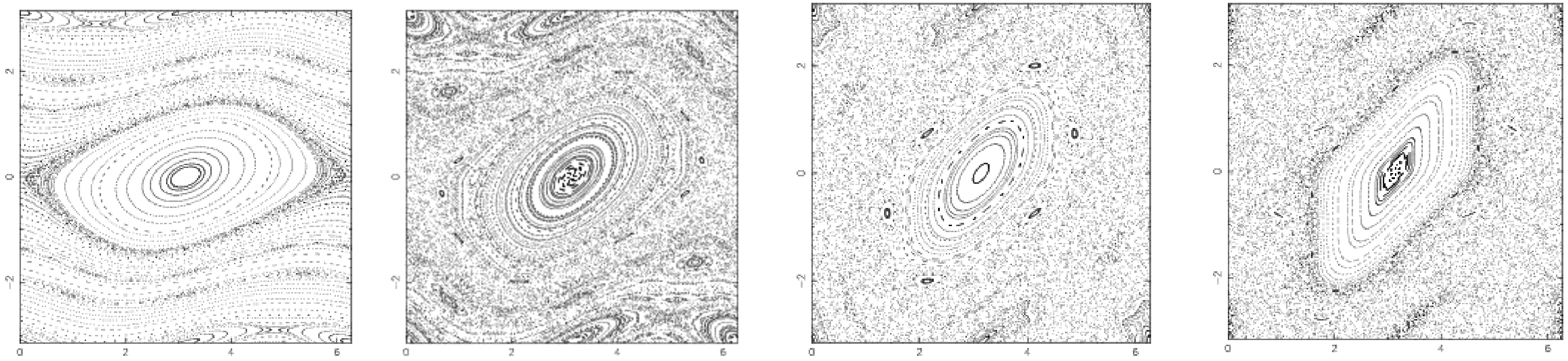

Chirikov, B. V. "A Universal Instability of Many-Dimensional Oscillator Systems." **Phys. Rep.** 52, 264-379, 1979.

*R.Z. Sagdeev, D.A. Usikov, G.M. Zaslavsky, **Nonlinear Physics, from the Pendulum to Turbulence and Chaos**, **Harwood Academic Publishers**, 1988.

Analyitcal treatment of dynamic apertures of multipoles

$$H=\frac{p^2}{2}+\frac{K(s)}{2}x^2+\frac{1}{m!B_0\rho}\frac{\partial^{m-1}B_z}{\partial x^{m-1}}x^mL\sum_{k=-\infty}^{\infty}\delta(s-kL)$$

$$B_z=B_0(1+xb_1+x^2b_2+x^3b_3+\cdots+x^{m-1}b_{m-1}+\cdots)$$

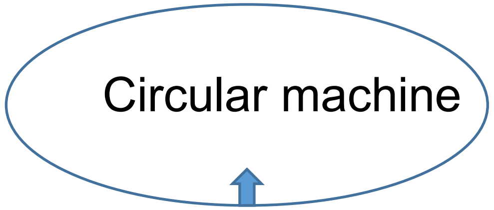

A nonlinear multipole

For one multipole $B_z=B_0x^{m-1}b_{m-1}$ m≥3

$$A_{dyna,2m}=\sqrt{2\beta_x(s)}\left(\frac{1}{m\beta_x^m(s(2m))}\right)^{\frac{1}{2(m-2)}}\left(\frac{\rho}{|b_{m-1}|L}\right)^{1/(m-2)}$$

For more independent multipoles

$$A_{\mathrm{dyna,total}}=\frac{1}{\sqrt{\sum_i\frac{1}{A^2_{\mathrm{dyna,sext},i}}+\sum_j\frac{1}{A^2_{\mathrm{dyna,oct},j}}+\sum_k\frac{1}{A^2_{\mathrm{dyna,deca},k}}+\cdots}}$$

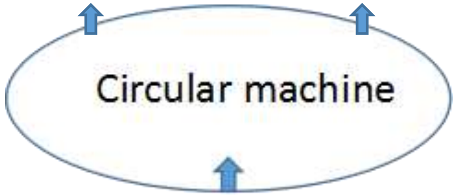

Many multipoles

$$H = \frac{p_x^2}{2} + \frac{K_x(s)}{2}x^2 + \frac{p_y^2}{2} + \frac{K_y(s)}{2}y^2 + \frac{1}{3!B\rho}\frac{\partial^2 B_z}{\partial x^2}(x^3 - 3xy^2)L\sum_{k=-\infty}^{\infty}\delta(s - kL)$$

$$H_{H\&H} = \frac{1}{2}\left(x^2 + p_x^2 + y^2 + p_y^2 + 2x^2y - \frac{2}{3}y^3\right)$$

Hénon and Heiles problem

Relation between X and Y

$$A_{dyna,sext,y} = \sqrt{\frac{\beta_x(s_1)}{\beta_y(s_1)}(A^2_{dyna,sext,x} - x^2)}$$

Héno-Heiles Problem

$$H_{\text{H\&H}} = \frac{1}{2}\left(x^2 + p_x^2 + y^2 + p_y^2 + 2y^2x - \frac{2}{3}x^3\right).$$

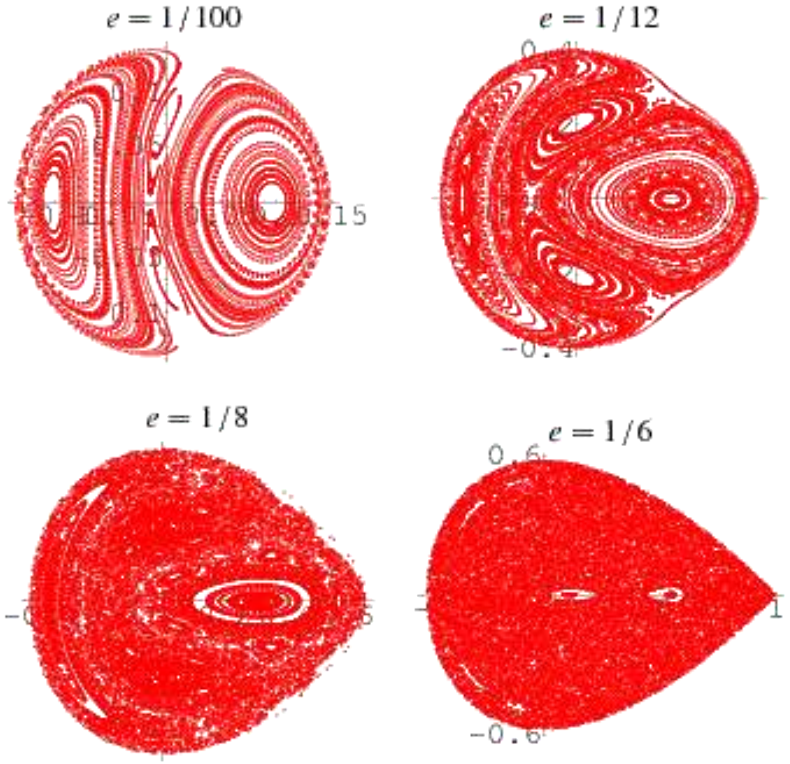

Hénon, M. and Heiles, C. "The Applicability of the Third Integral of Motion: Some Numerical Experiments." **Astron. J.** 69, 73-79, 1964.

Super-ACO lattice as an example

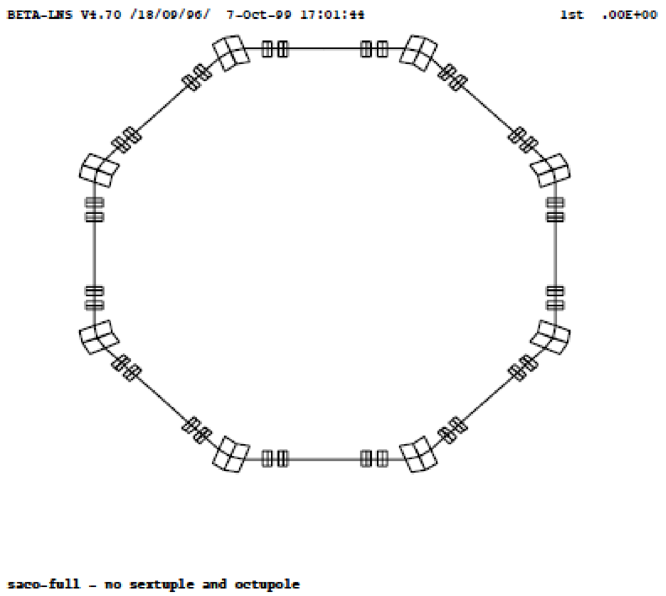

Figure 1.1: The schematic layout of Super-ACO.

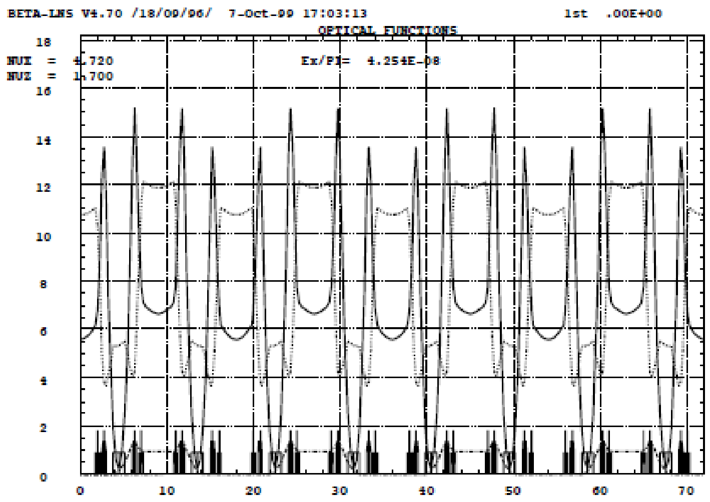

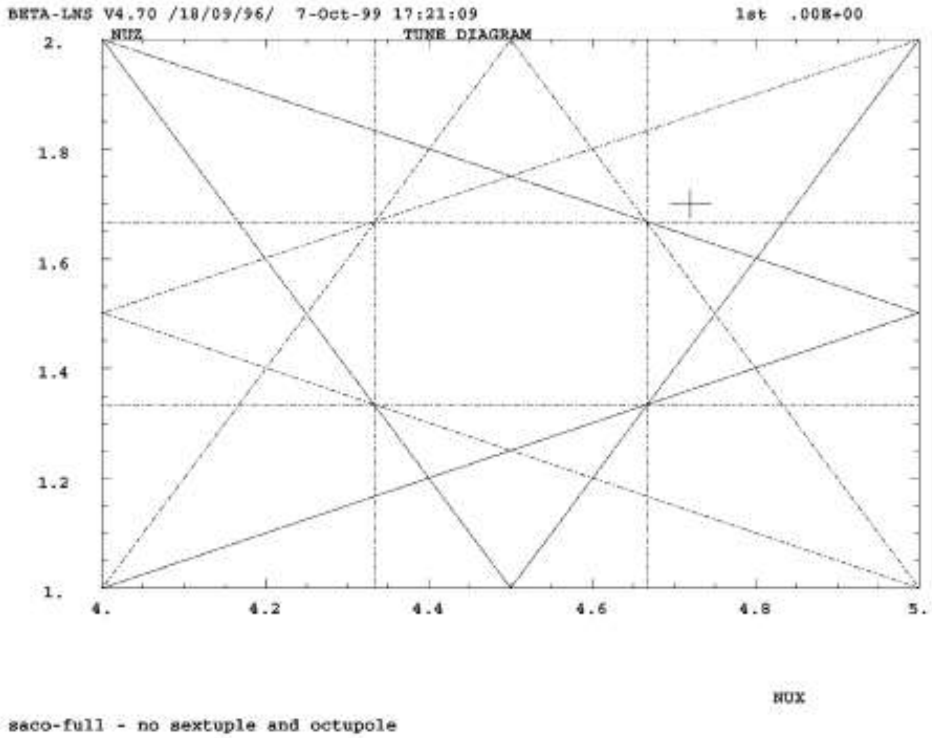

Fig. 3. The tune diagram of the third order of Super-ACO, where the cross indicates the working point of the machine.

Super-ACO lattice comparison results of analyical and numerical estimations on the dynamic apertures due to multipoles

Table 1
Summary of parameters

Case	Multipole strength	Beta function (m)
1	$S(s_1) = 2\ (1/\mathrm{m}^2)$	$\beta_x(s_1) = 13.6$
2	$O(s_1) = 10\ (1/\mathrm{m}^3)$	$\beta_x(s_1) = 13.6$
3	$D(s_1) = 1000\ (1/\mathrm{m}^4)$	$\beta_x(s_1) = 13.6$
4	$S(s_1) = 2\ (1/\mathrm{m}^2)$, $O(s_1) = 62\ (1/\mathrm{m}^3)$	$\beta_x(s_1) = 13.6$
5	$S(s_1) = 2\ (1/\mathrm{m}^2)$, $O(s_2) = 62\ (1/\mathrm{m}^3)$	$\beta_x(s_1) = 13.6$, $\beta(s_2) = 15.18$
6	$S(s_{1,2,3,4}) = 2\ (1/\mathrm{m}^2)$	$\beta_x(s_{1,2,3,4}) = 13.6$, 15.18, 7.8, 6.8
8	$S(s_1) = 2\ (1/\mathrm{m}^2)$	$\beta_x(s_1)=12.42$, $\beta_x(0)=5.1$
9	$S(s_1) = 2\ (1/\mathrm{m}^2)$	$\beta_x(s_2) = 15.18$

Table 2
Summary of comparison results

Case	$A_{\mathrm{dyna,analy.}}$ (m)	$A_{\mathrm{dyna,numer.}}$ (m)
1	0.0385	0.04
2	0.055	0.054
3	0.022	0.024
4	0.0145	0.016
5	0.0138	0.0135
6	0.012	0.0135
8	0.021	0.02
9	$A_x = 0.0163$, $A_y = 0.031$	$A_x = 0.017$, $A_y = 0.034$

case 1

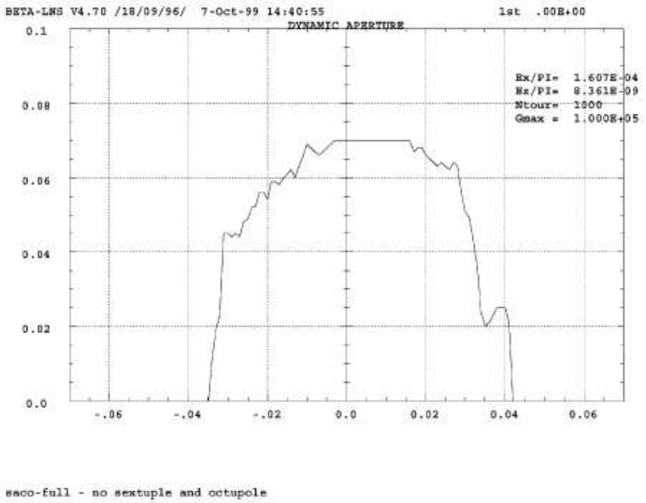

Fig. 4. The dynamic aperture plot ($S(s_1 = 1$ and $\beta_x(s_1) =$ 13.6 m).

case 2

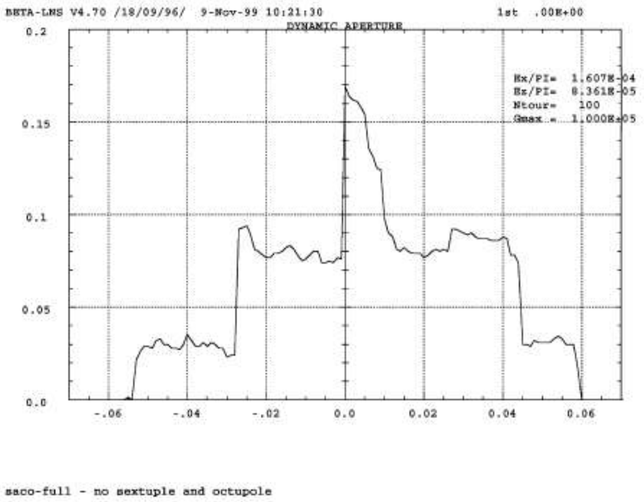

Fig. 6. The dynamic aperture plot ($O(s_1) = 10$ and $\beta_x(s_1) =$ 13.6 m).

case 1

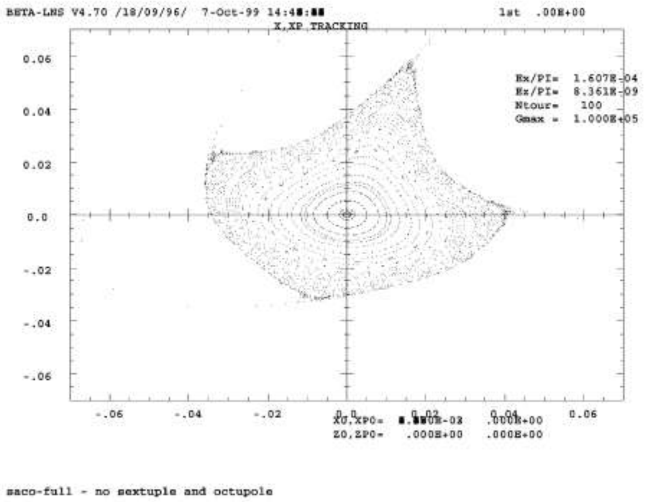

Fig. 5. The horizontal phase space ($S(s_1) = 1$ and $\beta_x(s_1) =$ 13.6 m).

case 2

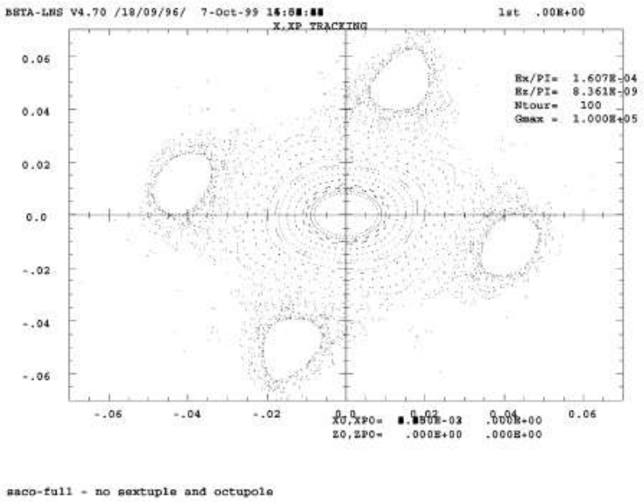

Fig. 7. The horizontal phase space ($O(s_1) = 10$ and $\beta_x(s_1) =$ 13.6 m).

case 3

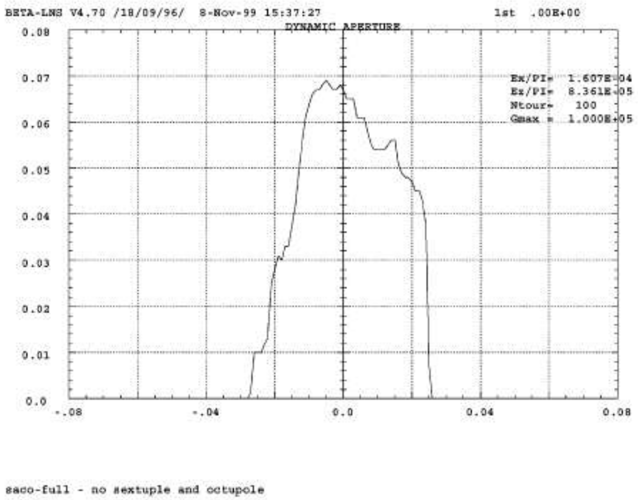

Fig. 8. The dynamic aperture plot ($D(s_1) = 1000$ and $\beta_x(s_1) = 13.6\,\mathrm{m}$).

case 4

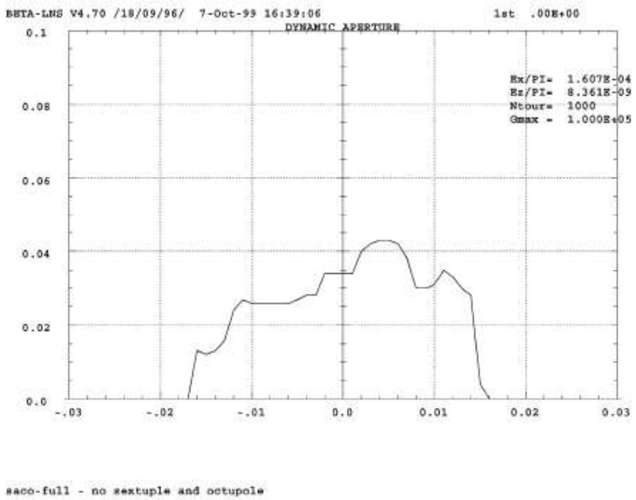

Fig. 10. The dynamic aperture plot ($S(s_1) = 2$, $O(s_1) = 62$, and $\beta_x(s_1) = 13.6\,\mathrm{m}$).

case 3

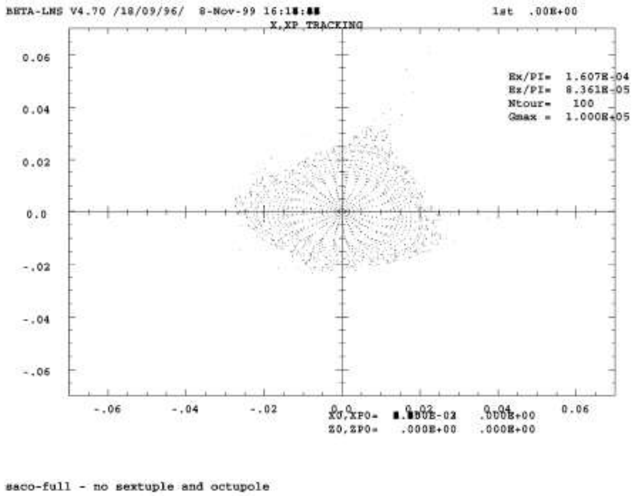

Fig. 9. The horizontal phase space ($D(s_1) = 1000$ and $\beta_x(s_1) = 13.6\,\mathrm{m}$).

case 4

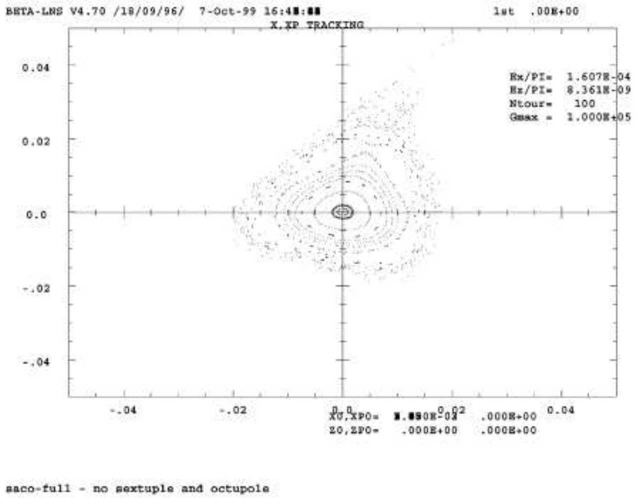

Fig. 11. The horizontal phase space ($S(s_1) = 2$, $O(s_1) = 62$, and $\beta_x(s_1) = 13.6\,\mathrm{m}$).

case 5

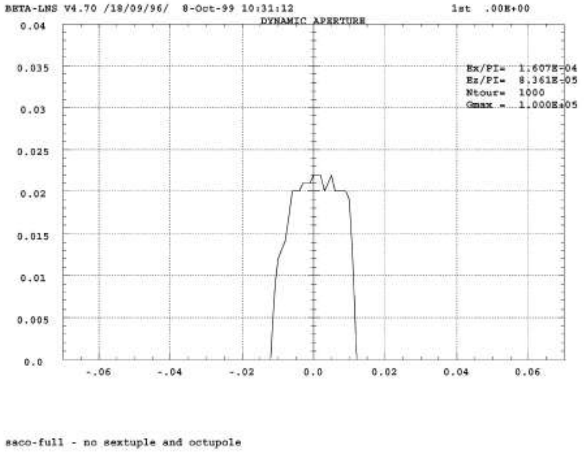

Fig. 12. The dynamic aperture plot ($S(s_1) = 2$, $O(s_2) = 62$, $\beta_x(s_1) = 13.6$ m, and $\beta_x(s_2) = 15.18$ m).

case 6

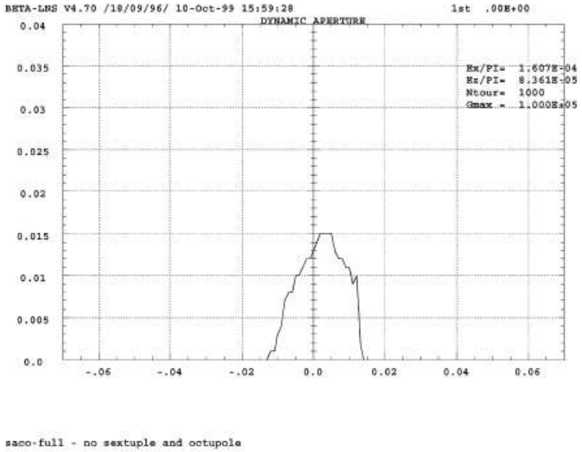

Fig. 14. The dynamic aperture plot ($S(s_{1,2,3,4}) = 2$, $\beta_x(s_1) = 13.6$ m, $\beta_x(s_2) = 15.18$ m, $\beta_x(s_3) = 7.8$ m, and $\beta_x(s_4) = 6.8$ m).

case 5

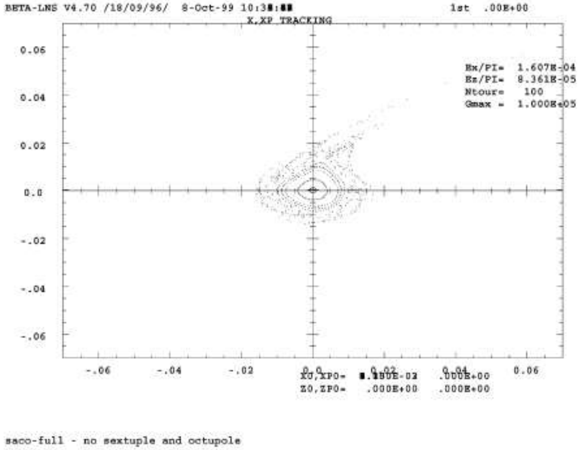

Fig. 13. The horizontal phase space ($S(s_1) = 2$, $O(s_2) = 62$, $\beta_x(s_1) = 13.6$ m, and $\beta_x(s_2) = 15.18$ m).

case 6

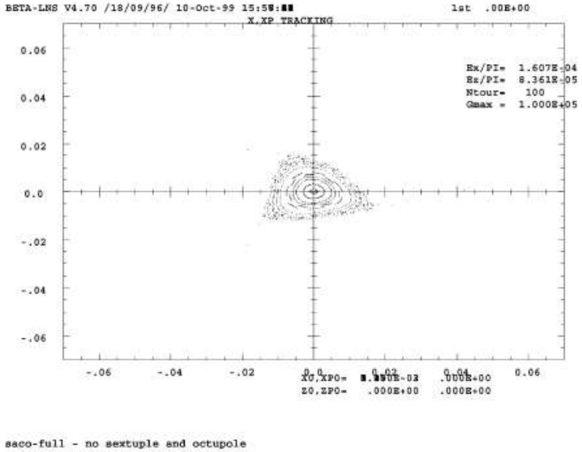

Fig. 15. The horizontal phase space ($S(s_{1,2,3,4}) = 2$, $\beta_x(s_1) = 13.6$ m, $\beta_x(s_2) = 15.18$ m, $\beta_x(s_3) = 7.8$ m, and $\beta_x(s_4) = 6.8$ m).

Super-ACO

Dynamic aperture of a sextupole vs strength

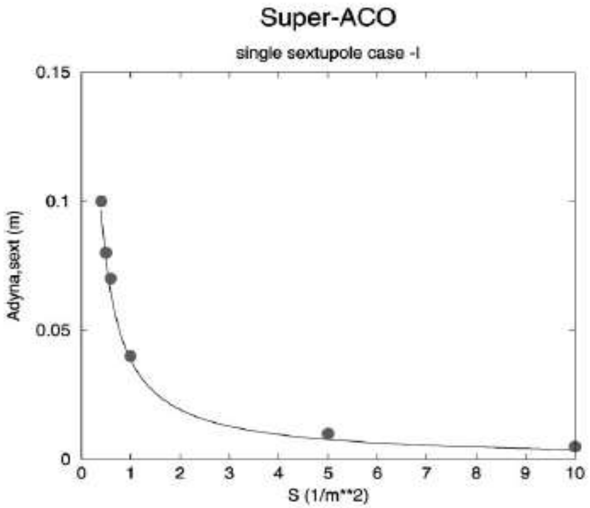

Fig. 16. The dynamic aperture of Super-ACO vs S ($S = b_2 L/\rho$) at s_1.

2D dynamic aperture of a sextupole: simulation

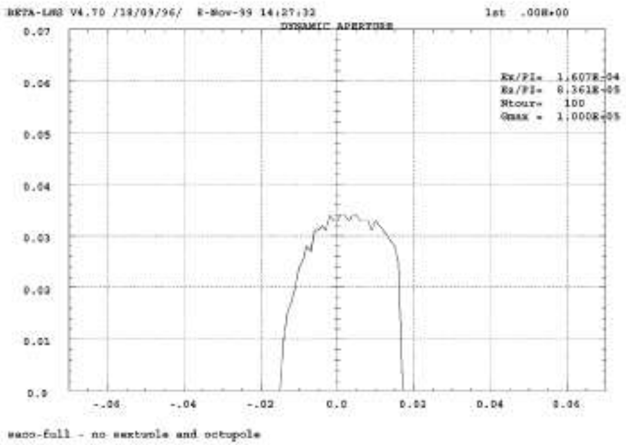

Fig. 22. The 2D dynamic aperture of Super-ACO with S = 2 located at s_2 with $\beta_x(s_2) = 15.18$ m and $\beta_y(s_2) = 4.26$ m.

Dynamic aperture of a octupole vs strength

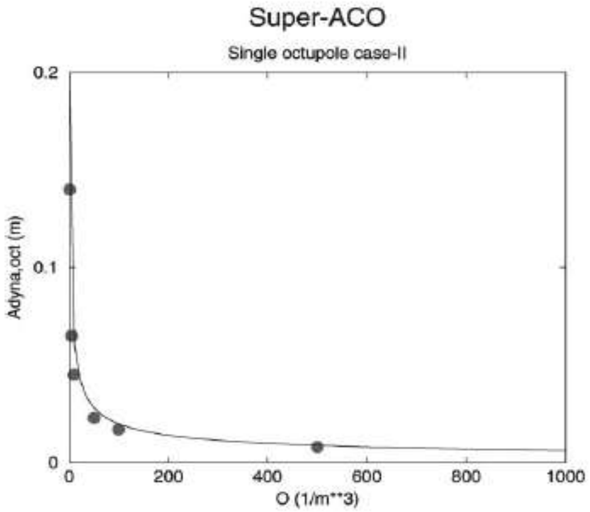

Fig. 17. The dynamic aperture of Super-ACO vs O ($O = b_3 L/\rho$) at s_2.

2D dynamic aperture of a sextupole: formula

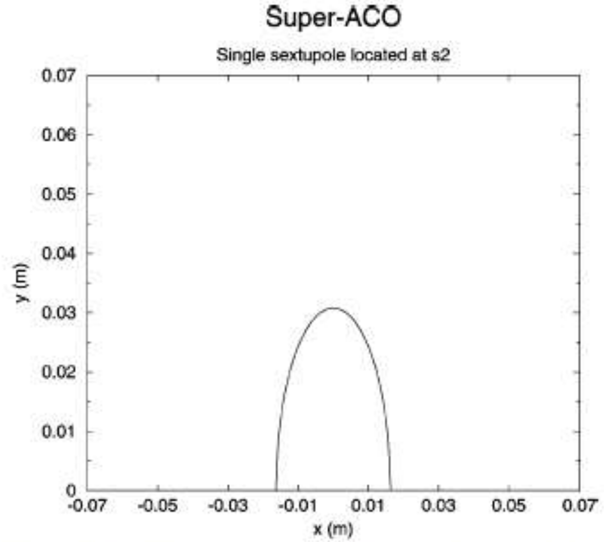

Fig. 23. The analytical estimation of the 2D dynamic aperture of Super-ACO with S = 2 located at s_2 with $\beta_x(s_2) = 15.8$ m and $\beta_y(s_2) = 4.26$ m.

Dynamic aperture of wigglers in a storage ring

A example of a sum of multipoles

$$B_x = \frac{k_x}{k_y} B_0 \sinh(k_x x) \sinh(k_y y) \cos(ks),$$

$$B_y = B_0 \cosh(k_x x) \cosh(k_y y) \cos(ks),$$

$$B_z = -\frac{k}{k_y} B_0 \cosh(k_x x) \sinh(k_y y) \sin(ks)$$

Wiggler fields

$$H_w = \frac{1}{2}\left(p_z^2 + (p_x - A_x \sin(ks))^2 + (p_y - A_y \sin(ks))^2\right)$$

$$A_x = \frac{1}{\rho_w k} \cosh(k_x x) \cosh(k_y y)$$

$$A_x = -\frac{k_x}{k_y} \frac{\sinh(k_x x) \sinh(k_y y)}{\rho_w k}$$

$$A_{N_w,y}(s) = \sqrt{\frac{3\beta(s)}{\beta_{y,m}^2}} \frac{\rho_w}{k_y \sqrt{L_w}},$$

$$A_{N_w,x}(s) = \sqrt{\frac{\beta_y(s)}{\beta_x(s)}(A_{N_w,y}(s)^2 - y^2)}.$$

$$A_{\text{total},y}(s) = \frac{1}{\sqrt{1/A_y(s)^2 + \sum_{j=1}^{M} 1/A_{j,\text{w},y}(s)^2}},$$

where N_w is the wiggler period number, λ_w is the wiggler period length, the wiggler length $L_w = N_w \lambda_w$, ρ_w is the radius of curvature of the wiggler peak magnetic field B_0, and $\rho_w = E_0/ecB_0$ with E_0 being the electron energy, and $\beta_{y,m}$ is the beta function value in the middle of the wiggler.

J. Gao, "Analytical estimation of dynamic apertures limited by the wigglers in storage rings", **Nuclear Instruments and Methods in Physics Research A** 516 (2004) 243–248

Comparison between the theoretical and numerical simulationresults of Super-ACO

Table 1
The dynamic apertures correspond to different ρ_w, where $A_{N_w,y,n}$ and $A_{N_w,y,a}$ correspond to numerical and analytical results, respectively

ρ_w (m)	$A_{N_w,y,n}$ (m)	$A_{N_w,y,a}$ (m)	$\beta_{y,m}$ (m)	λ_w (m)	L_w (m)
2.7	0.017	0.019	13	0.17584	3.5168
3	0.023	0.024	10.7	0.17584	3.5168
4	0.033	0.034	9.5	0.17584	3.5168

Table 2
The dynamic apertures correspond to different λ_w, where $A_{N_w,y,n}$ and $A_{N_w,y,a}$ correspond to numerical and analytical results, respectively

λ_w (m)	$A_{N_w,y,n}$ (m)	$A_{N_w,y,a}$ (m)	$\beta_{y,m}$ (m)	ρ_w (m)	L_w (m)
0.08792	0.016	0.017	9.55	4	3.5168
0.17584	0.033	0.034	9.5	4	3.5168
0.35168	0.067	0.067	9.5	4	3.5168

One wiggler case

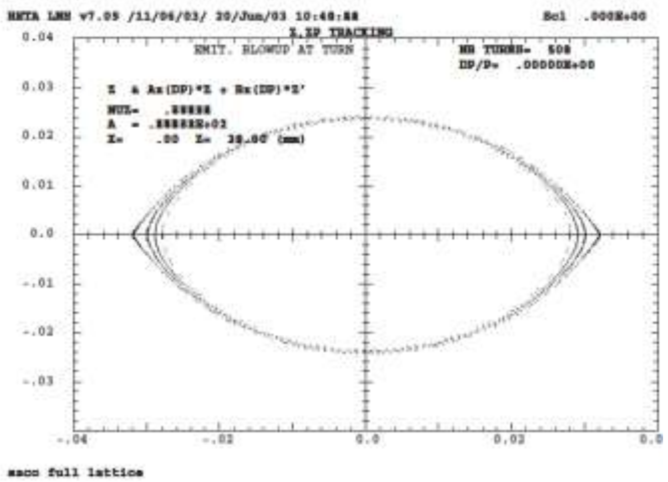

Fig. 5. The vertical phase space corresponds to the case of two wigglers.

When $\rho_w = 6$ m and $\beta_y(s) = \beta_{y,m} = 13.75$ m, one finds the vertical dynamic aperture limited by the two wigglers being 0.032 m numerically as shown in Fig. 5 and 0.03 m analytically calculated from Eqs. (19) and (23).

Two wiggler case

J. Gao, "Analytical estimation of dynamic apertures limited by the wigglers in storage rings", **Nuclear Instruments and Methods in Physics Research A** 516 (2004) 243–248

Bare lattice of Super-ACO

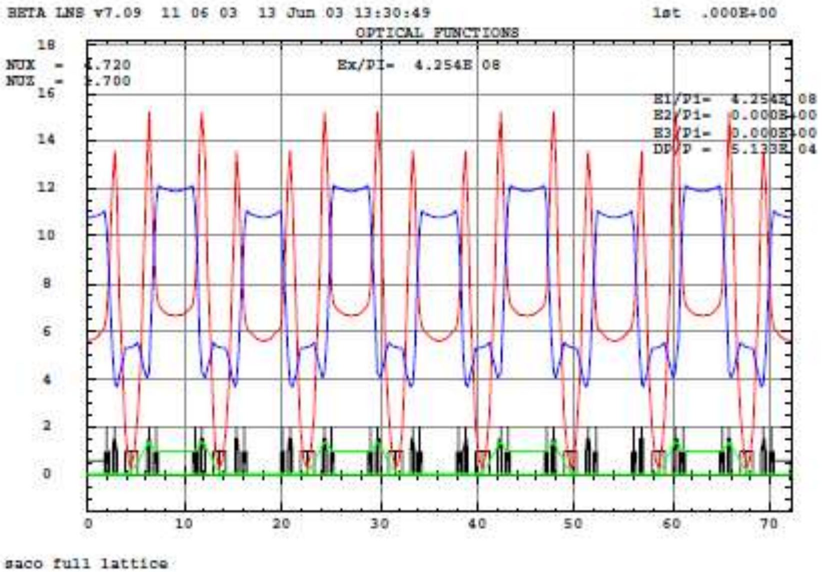

Fig. 1. The lattice of Super-ACO. The beta functions illustrated are those when the wiggler is switched off.

The first case in table 1

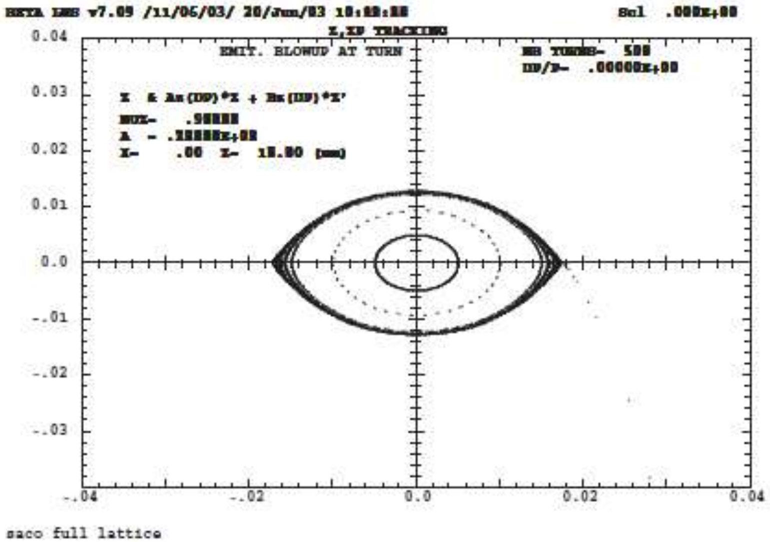

Fig. 2. The vertical phase space corresponds to the first case in Table 1.

The second case in table 1

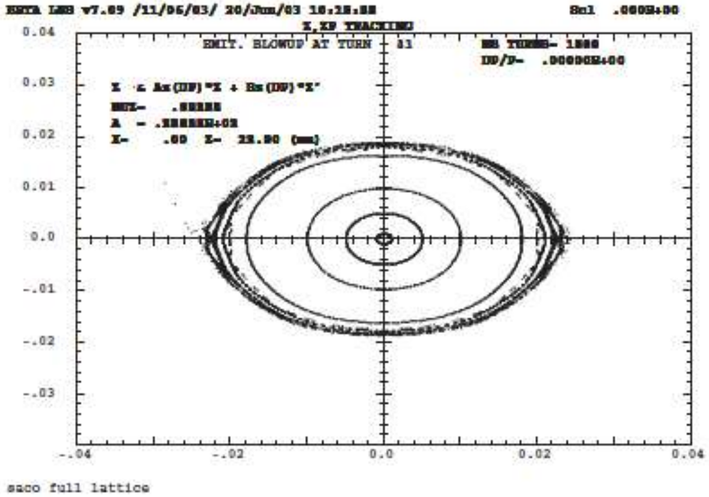

Fig. 3. The vertical phase space corresponds to the second case in Table 1.

The third case in table 1

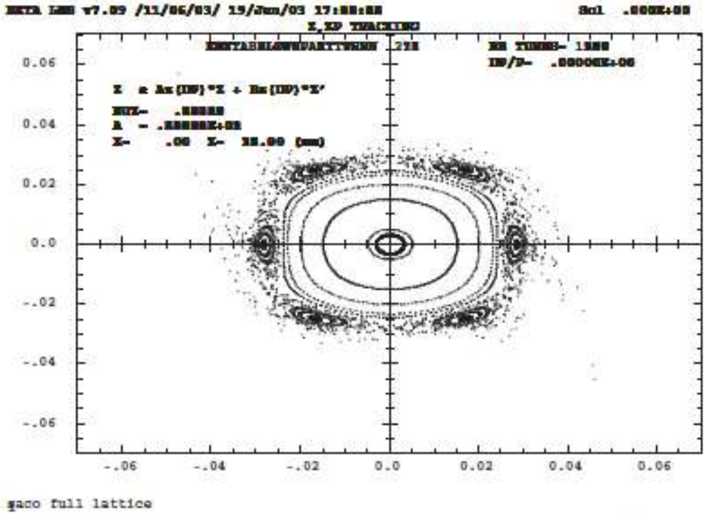

Fig. 4. The vertical phase space corresponds to the third case in Table 1.

Nonlinear beam-beam effects-1 (e+e-)

Basseti-Erskine formula for beam-beam induced transverse kicks

$$\delta y' + i\delta x' = -\frac{N_e r_e}{\gamma_*} f(x, y, \sigma_x, \sigma_y)$$

$$f(x,y,\sigma_x,\sigma_y) = \sqrt{\frac{2\pi}{\sigma_x^2-\sigma_y^2}} \times w\left(\frac{x+\mathrm{i}y}{\sqrt{2(\sigma_x^2-\sigma_y^2)}}\right) - \sqrt{\frac{2\pi}{\sigma_x^2-\sigma_y^2}} \times \exp\left(-\frac{x^2}{2\sigma_x^2}-\frac{y^2}{2\sigma_y^2}\right) w\left(\frac{\frac{\sigma_y}{\sigma_x}x+\mathrm{i}\frac{\sigma_x}{\sigma_y}y}{\sqrt{2(\sigma_x^2-\sigma_y^2)}}\right)$$

$$H_y = \frac{p_y^2}{2} + \frac{K_y(s)}{2}y^2 + \frac{N_e r_e}{\sqrt{2}\gamma_*}\left(\frac{1}{\sigma_x\sigma_y}y^2 - \frac{1}{12\sigma_x\sigma_y^3}y^4 + \frac{1}{120\sigma_x\sigma_y^5}y^6 - \frac{1}{1344\sigma_x\sigma_y^7}y^8 + \cdots\right) \times \sum_{k=-\infty}^{\infty}\delta(s-kL) \qquad \text{(FB)}, \qquad (38)$$

with $p_x = \mathrm{d}x/\mathrm{ds}$ and $p_y = \mathrm{d}y/\mathrm{ds}$.

J. Gao, “Analytical estimation ofthe beam–beam interaction limited dynamic apertures and lifetimes in e+e- circular colliders”, **Nuclear Instruments and Methods in Physics Research A** 463 (2001) 50–61

Nonlinear beam-beam effects-2 (e+e-)

$$\tau_{bb}=\frac{\tau_y}{2}\left(\frac{\langle y^2\rangle}{y_{\max}^2}\right)\exp\left(\frac{y_{\max}^2}{\langle y^2\rangle}\right)=\frac{\tau_y}{2}\left(\frac{\sigma_y(s)^2}{A_{\mathrm{dyna},y}(s)^2}\right)\exp\left(\frac{A_{\mathrm{dyna},y}(s)^2}{\sigma_y(s)^2}\right)$$

or

$$\tau^*_{bb,y}=\frac{\tau^*_y}{2}\left(\frac{16\gamma_*\sigma^2}{N_e r_e\beta_y(s_{\mathrm{IP}})}\right)^{-1}\exp\left(\frac{16\gamma_*\sigma^2}{N_e r_e\beta_y(s_{\mathrm{IP}})}\right)\quad\text{(RB)}$$

$$\tau^*_{bb,x}=\frac{\tau^*_x}{2}\left(\frac{6\gamma_*\sigma_x^2}{N_e r_e\beta_x(s_{\mathrm{IP}})}\right)^{-1}\exp\left(\frac{6\gamma_*\sigma_x^2}{N_e r_e\beta_x(s_{\mathrm{IP}})}\right)\quad\text{(FB)}$$

$$\tau^*_{bb,y}=\frac{\tau^*_y}{2}\left(\frac{3\sqrt{2}\gamma_*\sigma_x\sigma_y}{N_e r_e\beta_y(s_{\mathrm{IP}})}\right)^{-1}\exp\left(\frac{3\sqrt{2}\gamma_*\sigma_x\sigma_y}{N_e r_e\beta_y(s_{\mathrm{IP}})}\right)\quad\text{(FB)}$$

$$\tau^*_{bb,y}=\frac{\tau^*_y}{2}\left(\frac{4}{\pi\xi^*_y}\right)^{-1}\exp\left(\frac{4}{\pi\xi^*_y}\right)\quad\text{(RB)}$$

$$\tau^*_{bb,x}=\frac{\tau^*_x}{2}\left(\frac{3}{\pi\xi^*_x}\right)^{-1}\exp\left(\frac{3}{\pi\xi^*_x}\right)\quad\text{(FB)}$$

$$\tau^*_{bb,y}=\frac{\tau^*_y}{2}\left(\frac{3}{\sqrt{2}\pi\xi^*_y}\right)^{-1}\exp\left(\frac{3}{\sqrt{2}\pi\xi^*_y}\right)\quad\text{(FB).}$$

More generally, one has

$$\tau^*_{bb,2m,y}=\frac{\tau^*_y}{2}\left(\frac{2^{(m-2)/2}C_{m,\mathrm{RB}}}{4\pi\sqrt{m}\xi^*_y}\right)^{-2/m-2}\exp\left(\left(\frac{2^{(m-2)/2}C_{m,\mathrm{RB}}}{4\pi\sqrt{m}\xi^*_y}\right)^{2/m-2}\right)\quad\text{(RB)}$$

$$\tau^*_{bb,2m,x}=\frac{\tau^*_x}{2}\left(\frac{2^{(m-2)/2}C_{m,\mathrm{FB},x}}{\pi2\sqrt{m}\xi^*_y}\right)^{-2/m-2}\exp\left(\left(\frac{2^{(m-2)/2}C_{m,\mathrm{FB},x}}{\pi2\sqrt{m}\xi^*_x}\right)^{2/m-2}\right)\quad\text{(FB)}$$

Nonlinear beam-beam effects-3 (e+e-)

$$\xi_x^* = \frac{N_e r_e \beta_{x,\mathrm{IP}}}{2\pi\gamma^* \sigma_x(\sigma_x + \sigma_y)}$$

$$\xi_y^* = \frac{N_e r_e \beta_{y,\mathrm{IP}}}{2\pi\gamma^* \sigma_y(\sigma_x + \sigma_y)}$$

Dynamic apertures limited by nonlinear beam-beam effects

$$\frac{A_{\mathrm{dyna},8,y}(s)}{\sigma_*(s)} = \left(\frac{16\gamma_*\sigma^2}{N_e r_e \beta_y(s_{\mathrm{IP}})}\right)^{1/2} \quad \text{(RB)} \qquad = \left(\frac{4}{\pi\xi_y^*}\right)^{1/2}$$

$$\frac{A_{\mathrm{dyna},8,x}(s)}{\sigma_{*,x}(s)} = \left(\frac{6\gamma_*\sigma_x^2}{N_e r_e \beta_x(s_{\mathrm{IP}})}\right)^{1/2} \quad \text{(FB)} \qquad = \left(\frac{3}{\pi\xi_x^*}\right)^{1/2}$$

$$\frac{A_{\mathrm{dyna},8,y}(s)}{\sigma_{*,y}(s)} = \left(\frac{3\sqrt{2}\gamma_*\sigma_x\sigma_y}{N_e r_e \beta_y(s_{\mathrm{IP}})}\right)^{1/2} \quad \text{(FB).} \quad = \left(\frac{3}{\sqrt{2}\pi\xi_y^*}\right)^{1/2}$$

Nonlinear beam-beam effects-4 (e+e-)

More generally, one has

$$\tau^*_{bb,2m,y} = \frac{\tau^*_y}{2}\left(\frac{2^{(m-2)/2}C_{m,\mathrm{RB}}}{4\pi\sqrt{m}\xi^*_y}\right)^{-2/m-2} \exp\left(\left(\frac{2^{(m-2)/2}C_{m,\mathrm{RB}}}{4\pi\sqrt{m}\xi^*_y}\right)^{2/m-2}\right) \quad (\mathrm{RB})$$

$$\tau^*_{bb,2m,x} = \frac{\tau^*_x}{2}\left(\frac{2^{(m-2)/2}C_{m,\mathrm{FB},x}}{\pi 2\sqrt{m}\xi^*_y}\right)^{-2/m-2} \exp\left(\left(\frac{2^{(m-2)/2}C_{m,\mathrm{FB},x}}{\pi 2\sqrt{m}\xi^*_x}\right)^{2/m-2}\right) \quad (\mathrm{FB})$$

$$\tau^*_{bb,2m,y} = \frac{\tau^*_y}{2}\left(\frac{2^{(m-2)/2}C_{m,\mathrm{FB},y}}{\pi\sqrt{2m}\xi^*_y}\right)^{-2/m-2} \exp\left(\left(\frac{2^{(m-2)/2}C_{m,\mathrm{FB},y}}{\pi\sqrt{2m}\xi^*_y}\right)^{2/m-2}\right) \quad (\mathrm{FB}).$$

$$\xi^{\mathrm{RB}}_{y,\max} = \frac{4\sqrt{2}}{3}\xi^{\mathrm{FB}}_{y,\max} = 1.89\xi^{\mathrm{FB}}_{y,\max}$$ Round beam vs flat beam

and

$$\xi^{\mathrm{FB}}_{x,\max} = \sqrt{2}\xi^{\mathrm{FB}}_{y,\max}.$$

J. Gao, “Analytical estimation ofthe beam–beam interaction limited dynamic apertures and lifetimes in e+e- circular colliders”, **Nuclear Instruments and Methods in Physics Research A** 463 (2001) 50–61

Parasitic crossing beam-beam effects

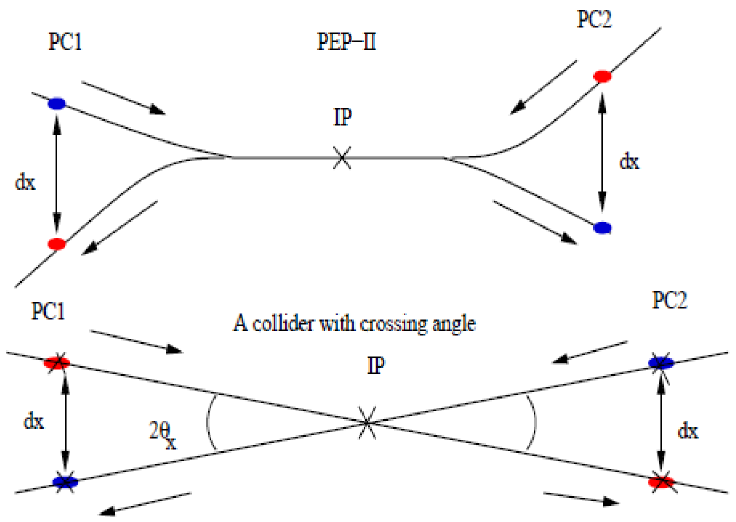

$$\tau_{PC,y,RB} = \frac{\tau_y}{2}\left(\mathcal{R}_{y,PC,RB}\right)^{-1}\exp\left(\mathcal{R}_{y,PC,RB}\right)$$

$$= \frac{\tau_y}{2}\left(\frac{4}{\pi\xi_{PC,y}}\right)^{-1}\exp\left(\frac{4}{\pi\xi_{PC,y}}\right)$$

with

$$\xi_{PC,y} = \frac{r_e N_e \beta_{PC,x}}{2\pi\gamma_* \Sigma_{PC}^2} = \frac{r_e N_e \beta_{PC,y}}{2\pi\gamma_* d_x^2}$$

$$\Sigma_{PC}, \Sigma_{PC} = \sqrt{d_x^2 + d_y^2}$$

J. Gao, ON PARASITIC CROSSINGS AND THEIR LIMITATIONS TO E+E− STORAGE RING COLLIDERS, **Proceedings of EPAC 2004**, Lucerne, Switzerland, p. 671-673 (2004)

J. Gao, “Analytical treatment of the nonlinear electron cloud effect and the combined effects with beam-beam and space charge nonlinear forces in storage rings”, **Chinese Physics C** Vol. 33, No. 2, Feb., 2009, 135-144

Beam-beam effects with crossing angle

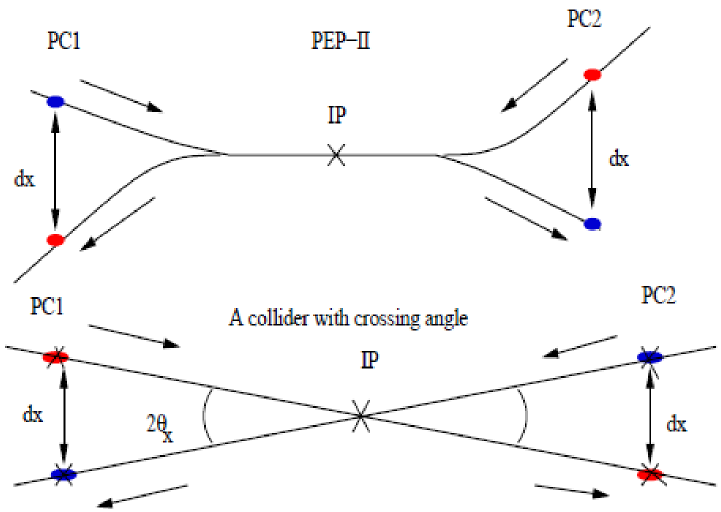

$$\mathscr{R}_{\text{syn-beta},x} = \frac{A_{\text{syn-beta},x}(s)^2}{\sigma_x(s)^2} = \frac{2}{3\pi^2}\left(\frac{1}{\xi_x^* \Phi}\right)^2$$

where $\Phi = (\sigma_z/\sigma_x)\phi$ is Piwinski angle.

J. Gao, "Analytical estimation of the effects of crossing angle on the luminosity of an e+e- circular collider", **Nuclear Instruments and Methods in Physics Research A** 481 (2002) 756–759

J. Gao, "Analytical treatment of the nonlinear electron cloud effect and the combined effects with beam-beam and space charge nonlinear forces in storage rings", **Chinese Physics C** Vol. 33, No. 2, Feb., 2009, 135-144

Space charge nonlinear effects

$$\left(\frac{A_{\text{total},sc,y}(s)}{\sigma_y(s)}\right)^2 = \frac{3}{\sqrt{2}\pi\xi_{sc}}$$

$$\xi_{sc,y} = -\frac{r_{\mathrm{e}} N_{\mathrm{e}} \beta_{\mathrm{av},y}}{2\pi\gamma\sigma_y(\sigma_x+\sigma_y)}\left(\frac{L}{\sqrt{2\pi}\beta^2\gamma^2\sigma_z}\right)$$

J. Gao, “Analytical treatment of the nonlinear electron cloud
effect and the combined effects with beam-beam and space charge nonlinear forces in storage rings”, **Chinese Physics C** Vol. 33, No. 2, Feb., 2009, 135-144

J. Gao, Theoretical analysis of the limitation from the nonlinear space charge forces to TESLA damping ring, **TESLA 2003-12**

TESLA

TESLA COLLABORATION

Theoretical Analysis on the Limitation from the Nonlinear Space Charge Forces to TESLA Damping Ring

J. Gao

LAL IN2P3-CNRS Orsay

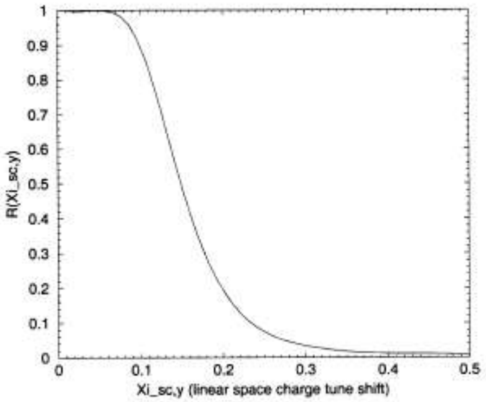

CERN LIBI

CM-I

February 2003, TESLA 2003-12

Electron cloud nonlinear effect

$$\xi'_{\mathrm{ec}}(s_0) = \frac{r_e N_{\mathrm{ec}} \beta_{+,y}(s_0)}{2\pi\gamma_+ \sigma_{+,y}(s_0)(\sigma_{+,x}(s_0) + \sigma_{+,y}(s_0))} \left(\frac{1}{2L_0}\right)$$

$$\left(\frac{A_{\mathrm{ec},y}}{\sigma_{+,y}}\right)^2 \approx \frac{3\sqrt{2}\gamma_+}{\pi r_{\mathrm{e}} \beta_{av,y} \rho_{\mathrm{ec}} L}$$

$$\rho_{\mathrm{ec}} = \frac{N_{\mathrm{ec}}}{2\pi\sigma_{\mathrm{av},+,x}\sigma_{\mathrm{av},+,y} L_0}$$

J. Gao, "Analytical treatment of the nonlinear electron cloud effect and the combined effects with beam-beam and space charge nonlinear forces in storage rings", **Chinese Physics C** Vol. 33, No. 2, Feb., 2009, 135-144

Combined beam-beam, space charge, electron cloud nonlinear effects

$$\mathcal{R}^2_{\mathrm{ec},y} = \left(\frac{A_{\mathrm{ec},y}}{\sigma_{+,y}}\right)^2 \approx \frac{3\sqrt{2}\gamma_+}{\pi r_{\mathrm{e}} \beta_{av,y} \rho_{\mathrm{ec}} L}, \qquad \rho_{\mathrm{ec}} = \frac{N_{\mathrm{ec}}}{2\pi \sigma_{\mathrm{av},+,x} \sigma_{\mathrm{av},+,y} L},$$

$$\mathcal{R}^2_{\mathrm{total},+,y} = \frac{1}{\frac{1}{\mathcal{R}^2_{bb,+,y}} + \frac{1}{\mathcal{R}^2_{\mathrm{ec},y}} + \frac{1}{\mathcal{R}^2_{sc,y}}},$$

$$\tau_{\mathrm{total},+,y} = \frac{\tau_{+,y}}{2} \left(\mathcal{R}^2_{\mathrm{total},+,y}\right)^{-1} \exp\left(\mathcal{R}^2_{\mathrm{total},+,y}\right)$$

J. Gao, “Analytical treatment of the nonlinear electron cloud effect and the combined effects with beam-beam and space charge nonlinear forces in storage rings”, **Chinese Physics C** Vol. 33, No. 2, Feb., 2009, 135-144

Analytical formulae for dynamic apertures with energy spread

WEPEA022 Proceedings of IPAC2013, Shanghai, China

ANALYTICAL ESTIMATIONS OF THE DYNAMIC APERTURES OF BEAMS WITH MOMENTUM DEVIATION AND APPLICATION IN FFAG*

Ming Xiao†, Jie Gao, IHEP, Beijing, China

$$H = \frac{p_\beta^2}{2} - (1-\Delta)\left(K_x + \Delta SD\right)\frac{x_\beta^2}{2} + (1-\Delta)S\frac{x_\beta^3}{6}$$

$$A_{dyna,sext,\Delta} = \frac{1}{1-\Delta}\sqrt{\frac{8\tilde{\beta}_x(s)}{3(B^2+C^2)}} = \Omega \times A_{dyna,sext} \tag{16}$$

Here we call Ω the modulation factor. It is clear to tell that the dynamic aperture for off-momentum particles is modulated by both the momentum deviation and the linear lattice's characteristic.

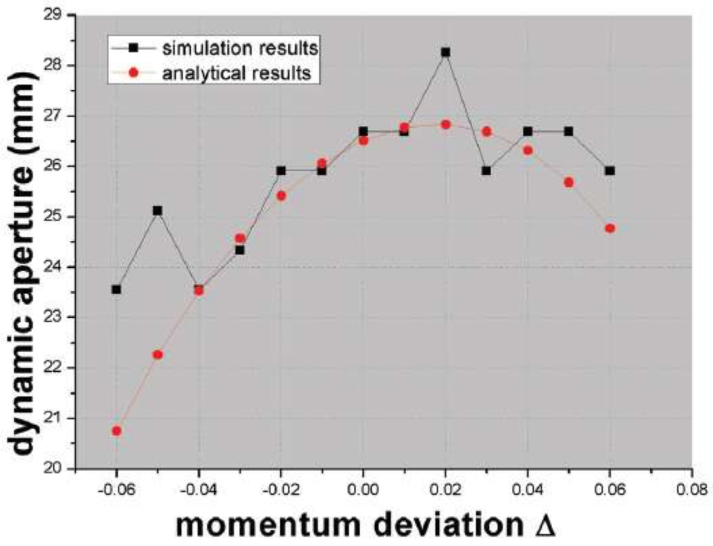

BEPCII DA

M. Xiao and J. Gao, "ANALYTICAL ESTIMATIONS OF THE DYNAMIC APERTURES OF BEAMS WITH MOMENTUM DEVIATION AND APPLICATION IN FFAG", WEPEA022 **Proceedings of IPAC2013**, Shanghai, China, p. 2546-2548

Luminosity from Colliding Beams

- For equally intense Gaussian beams

Particles in a bunch

Collision frequency

Geometrical factor:
- crossing angle
- hourglass effect

- Expressing luminosity in terms of our usual beam parameters

$$L = f \frac{N_b{}^2}{4\pi\sigma_x\sigma_y} R$$

Transverse beam size (RMS)

ICFA mini workshop: Beam-Beam Effects in Circular Colliders
BB24， Sept. 2-5, 2024, EPFL, Switzerland
https://indico.cern.ch/event/1344947/sessions/518431/#20240902

Beam-beam effect is an important issue for colliders

Luminosity of Circular Colliders

$$L[\mathrm{cm}^{-2}\mathrm{s}^{-1}] = 2.17\times10^{34}(1+r)\xi_y \frac{E[\mathrm{GeV}]I[\mathrm{A}]}{\beta_y[\mathrm{cm}]}$$

In ACO it is found that ξ_y has a maximum value

where

$$\boxed{\xi_y = \frac{r_e N_e \beta_y}{2\pi\sigma_y(\sigma_x+\sigma_y)}}$$

For exampe, for BEPCII at 1.89 $\xi_{\mathrm{ymax}} = 0.04$

Analytical expression for the maximum value of $\xi_{\mathrm{y,max}}$ is the keystone of a circular colliders both for lepton and hadron one

$$\xi_y = \frac{r_e N_e \beta_y}{2\pi\sigma_y(\sigma_x + \sigma_y)}$$

Maximum Beam-beam tune shift analytical expressions for lepton and hadron circular colliders

For example: BEPCII@ 1.89GeV
$\xi_{y,max},\ theory = 0.04$
$\xi_{y,max},\ exp = 0.04$

For lepton collider (flat beam and head-on):

$$\xi_{y,\max} = \frac{2845}{2\pi}\sqrt{\frac{T_0}{\tau_y \gamma N_{IP}}} \qquad \xi_{y,\max} = \frac{2845\gamma}{1}\sqrt{\frac{r_e}{6\pi R N_{IP}}}$$

r_e is electron radius
γ is normalized energy
R is the dipole bending radius
N_{IP} is number of interaction points

$$\xi_{x,\max} = \sqrt{2}\xi_{y,\max}$$

J. Gao, Emittance growth and beam lifetime limitations due to beam-beam effects in e+e- storage rings, **Nuclear Instruments and Methods in Physics Research A** 533 (2004) 270–274

J. Gao, **Nuclear Instruments and Methods in Physics Research A** 463 (2001) 50–61

For hadron collider (round beam and hean-on):

Keystones

$$\xi_{\max} = \frac{2845\gamma}{f(x)}\sqrt{\frac{r_p}{6\pi R N_{IP}}} \times \frac{4}{3}\sqrt{2}$$

where r_p is proton radius

$$f(x) = 1 - \frac{2}{\sqrt{2\pi}}\int_0^x \exp\left(-\frac{t^2}{2}\right)dt$$

$$x^2 = \frac{4f(x)}{\pi\xi_{\max}N_{IP}} = \frac{4f^2(x)}{2845\pi\gamma}\sqrt{\frac{6\pi R}{r_p N_{IP}}}$$

J. Gao, "Review of some important beam physics issues in electron positron collider designs", **Modern Physics Letters A**, Vol. 30, No. 11 (2015) 1530006 (20 pages)

For example: LHC@ 13TeV
$\xi_{y,max},\ theory = 0.005$
$\xi_{y,max},\ exp = 0.0045$

J. Gao, et al, "Analytical estimation of maximum beam-beam tune shifts for electron-positron and hadron circular colliders", Proceedings of ICFA Workshop on High Luminosity Circular e+e- Colliders – Higgs Factory, 2014

$$\xi_y \leqslant \xi_{y,\mathrm{max,em,flat}} = \frac{h\mathscr{H}_0\gamma}{F}\sqrt{\frac{r_e}{6\pi R N_{\mathrm{IP}}}} \tag{16}$$

or, in general case, one has

$$\xi_y \leqslant \xi_{y,\mathrm{max,em,flat}} = \frac{h\mathscr{H}_0}{2\pi F}\sqrt{\frac{T_0}{\tau_y\gamma N_{\mathrm{IP}}}} \tag{17}$$

where h is a constant used to quantify how the denominator in Eq. (11) is approaching to zero, defining $H_0 = h\mathscr{H}_0$, one has $H_0 \approx 2845$, which is not a derived value, but obtained by comparing with experimental results, R is the local dipole bending radius, and F is expressed as follows:

$$F = \frac{\sigma_s}{\sqrt{2}\beta_{y,*}}\left(1+\left(\frac{\beta_{y,*}}{\sigma_s}\right)^2\right)^{1/2}. \tag{18}$$

Table 1
Machine parameters

Machine	N_{IP}	Energy (GeV)	γ	τ_y (ms)	T_0 (μs)	Φ_{Piwin}
DAFNE	1	0.51	10^3	36	0.325	0.22
BEPC	1	1.89	3.7×10^3	28	0.8	0
PEP-II(L)	1	3.12	6.12×10^3	62	7.33	0
KEKB(L)	1	3.5	6.86×10^3	43	10.05	0.69
KEKB(H)	1	8	1.57×10^4	46	10.05	0.69
PEP-II(H)	1	8.99	1.76×10^4	37	7.33	0
LEP-100	4	45	8.82×10^4	38	88.9	0
LEP-200	4	80.5	1.58×10^5	5	88.9	0

J. Gao, Emittance growth and beam lifetime limitations due to beam–beam effects in storage ring colliders, Nuclear Instruments and Methods in Physics Research A 533 (2004) 270–274

Comparison electron positron circular collider beam-beam limit Formulae and experimental results (~head-on flat beam collision)

Table 1
Machine parameters

Machine	N_{IP}	Energy (GeV)	γ	τ_y (ms)	T_0 (μs)	Φ_{Piwin}
DAFNE	1	0.51	10^3	36	0.325	0.22
BEPC	1	1.89	3.7×10^3	28	0.8	0
PEP-II(L)	1	3.12	6.12×10^3	62	7.33	0
KEK B(L)	1	3.5	6.86×10^3	43	10.05	0.69
KEK B(H)	1	8	1.57×10^4	46	10.05	0.69
PEP-II(H)	1	8.99	1.76×10^4	37	7.33	0
LEP-100	4	45	8.82×10^4	38	88.9	0
LEP-200	4	80.5	1.58×10^5	5	88.9	0

Table 2
Theoretical maximum and experimentally achieved beam–beam parameters

Machine	$\xi_{y,\max,\text{theory}}$	$\xi_{y,\max,\text{exp}}$
DAFNE	0.043	0.02
BEPC	0.04	0.04
PEP-II(L)	0.063	0.06
KEKB(L)	0.084	0.069
KEKB(H)	0.053	0.052
PEP-II(H)	0.048	0.048
LEP-I	0.037	0.033
LEP-II	0.076	0.079

J. Gao, Emittance growth and beam lifetime limitations due to beam–beam effects in electron positron storage ring colliders, **Nuclear Instruments and Methods in Physics Research A** 533 (2004) 270–274

Hadron collider beam-beam limit formulae (pp, round beam)

Eq. I $$\xi_{h,y,\max} = \frac{H_0 \gamma}{f(x_*)}\sqrt{\frac{r_h}{6\pi R N_{\mathrm{IP}}}} \times \frac{4}{3}\sqrt{2}$$

H_0 ~2845,

Eq. II $$\xi_{h,y,\max} = \frac{H_0}{2\pi f(x_*)}\sqrt{\frac{T_0}{\tau_y \gamma N_{\mathrm{IP}}}} \times \frac{4}{3}\sqrt{2}$$

Eq. I and Eq. II are equivalent for isomagnetic lattice

Eqs. I and II with round proton beam collisions will be published in:
J. Gao, "The Status of the CEPC Project in EDR",
International Journal of Modern Physics A, submitted in 2025

$$f(x) = 1 - \frac{2}{\sqrt{2\pi}}\int_0^x \exp\left(-\frac{t^2}{2}\right)dt$$

$$x^2 = \frac{4f(x)}{\pi \xi_{y,\max} N_{\mathrm{IP}}}$$

$$x_*^2 = \frac{4f(x_*)^2}{H_0 \pi \gamma}\sqrt{\frac{6\pi R}{r_h N_{\mathrm{IP}}}}$$

f=1 corresponds electron positron colliders

Machine	E[TeV]	R[m]	N_{IP}	$\xi_{y,analy}$	$\xi_{y,meas}$	$\xi_{y,para}$
Tevatron	0.98	682	2	0.0026	0.0125	0.012
LHC	7	2801	3	0.0045	0.0045	0.005
SSC	22	9824	2	0.0081		0.0021
HL-LHC	7	2801	2	0.0060		0.0086
FCC-hh	50	10663	2	0.0128		0.015
SPPC	62.5	10415	2	0.0147		0.015

J. Gao, "Emittance Growth and Beam Lifetime due to Beam-Beam Interaction in a Circular Collider", Personal note, 2004 (LAL, Orsay)

J. Gao, "Review of some important beam physics issues in electron positron collider designs", **Modern Physics Letters A** Vol. 30, No. 11 (2015) 1530006 (20 pages)

J. Gao† , M. Xiao, F. Su, S. Jin, D. Wang, Y.W. Wang, S. Bai, T.J. Bian, "ANALYTICAL ESTIMATION OF MAXIMUM BEAM-BEAM TUNE SHIFTS FOR ELECTRON-POSITRON AND HADRON CIRCULAR COLLIDERS", **HF2014 Proceddings** (2014)

Analytical formulae for the luminosity of electron-positron circular collider with flat beam crab-waist crossing

By using following relations One could get more equivalent formulae:

$I_b=P_b/U_0$

$U_0=C\gamma E^4/R$

$C\gamma=8.85*10^{-5}\mathrm{mGeV}^{-3}$

$R=r_0C_0/2\pi$

where R is local bending radius, r_0 is dipole filling factor, C_0 is collider circumference

$$L[\mathrm{cm}^{-2}\mathrm{s}^{-1}] = 2.17\times10^{34}(1+r)\xi_{y\mathrm{max}}\frac{E[\mathrm{GeV}]I[\mathrm{A}]}{\beta_y[\mathrm{cm}]}e^{\frac{\sqrt{\Phi p}}{3.22}}(1+0.000505*\Phi p^2) \quad \text{Eq. A}$$

$$L_{\max}[\mathrm{cm}^{-2}\mathrm{s}^{-1}] = \frac{0.158\times10^{34}(1+r)}{\beta_y^*[\mathrm{mm}]}I_b[\mathrm{mA}]\sqrt{\frac{U_0[\mathrm{GeV}]}{N_{\mathrm{IP}}}}e^{\frac{\sqrt{\Phi p}}{3.22}}(1+0.000505*\Phi p^2) \quad \text{Eq. B}$$

$$L_{\max}[\mathrm{cm}^{-2}\mathrm{s}^{-1}] = \frac{0.158\times10^{34}(1+r)}{\beta_y^*[\mathrm{mm}]}\sqrt{\frac{I_b[\mathrm{mA}]P_b[\mathrm{MW}]}{N_{\mathrm{IP}}}}e^{\frac{\sqrt{\Phi p}}{3.22}}(1+0.000505*\Phi p^2) \quad \text{Eq. C}$$

$$L_{\max}[cm^{-2}\ s^{-1}]=0.158\times10^{34}\frac{(1+r)}{\beta_y[\mathrm{mm}]}\sqrt{\frac{R[m]}{C_\gamma[mGeV^3]N_{IP}}}(P_b[\mathrm{MW}]/E[GeV]^2)e^{\frac{\sqrt{\Phi_p}}{3.22}}(1+0.000505*\Phi_p^2) \quad \text{Eq. D}$$

Φp is *Piwinski angle* $=(\sigma_z/\sigma_x)\tan(\Theta/2)$, and Θ is the crossing angle

Eq. A, B, C, D are equivalent for isomagnetic lattice

where $r=\sigma_{y,*}/\sigma_{x,*}$, N_b is the number of bunches inside a beam, I_b is the average current of a bunch, and $I_{\mathrm{beam}}=N_bI_b$.

Eqs. A, B, C and D are formulae with crab-wait corrections will be published in:
J. Gao, "The Status of the CEPC Project in EDR", International Journal of Modern Physics A, submitted in 2025

CEPC-SppC Physics Goals in TDR

Introduction

- **Circular Electron-Positron Collider (91, 160， 240 GeV, 360GeV)**
  - **Higgs Factory（10^6 Higgs）：**
    - Precision study of Higgs(m_H, J^{PC}, couplings)， Similar & complementary to Linear Colliders
    - Looking for hints of new physics
  - **Z & W factory（10^{10}~10^{12} Z^0）：**
    - precision test of SM
    - Rare decays ?
  - **Flavor factory: b, c, τ and QCD studies**
- **Super proton-proton Collider(~125 TeV)**
  - **Directly search for new physics beyond SM**
  - **Precision test of SM**
    - **e.g., h^3 & h^4 couplings**

The discoveries of Higgs boson around 125GeV at CERN on LHC on July 4, 2012 and the gravitation waves on LIGO in USA on February 11, 2016 provide unprecedented opportunities to our better understandings of mysterious universe

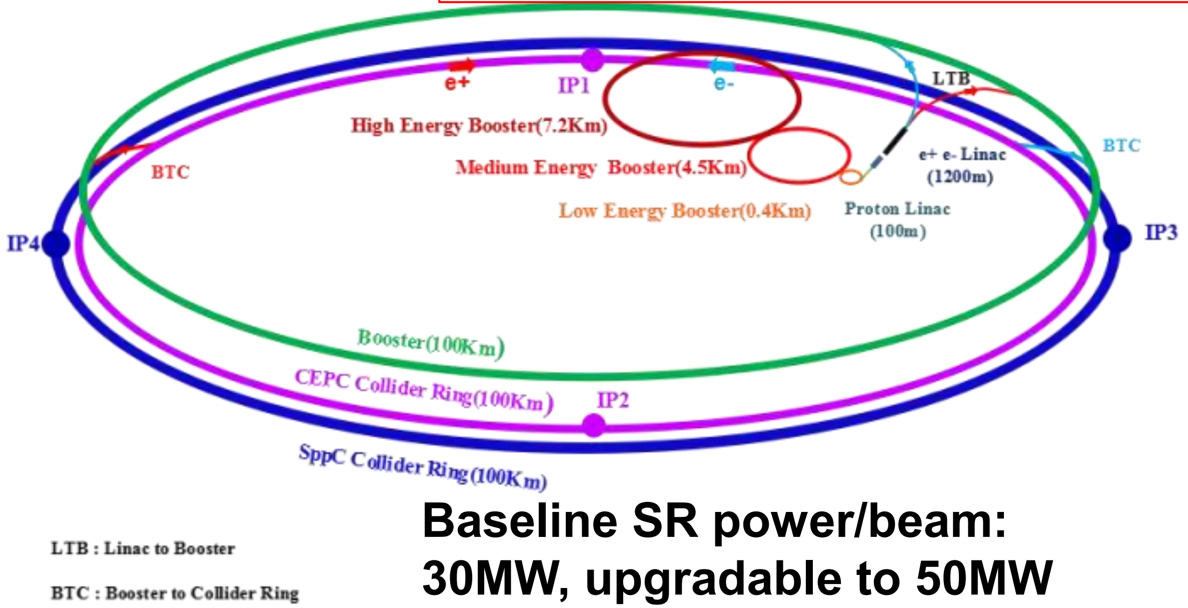

Baseline SR power/beam: 30MW, upgradable to 50MW

CEPC TDR Layout@30GeV Linac

CEPC as a Higgs Factory： H, W, Z, upgradable to tt-bar, followed by a SppC ~125TeV

30MW SR power per beam (upgradale to 50MW)

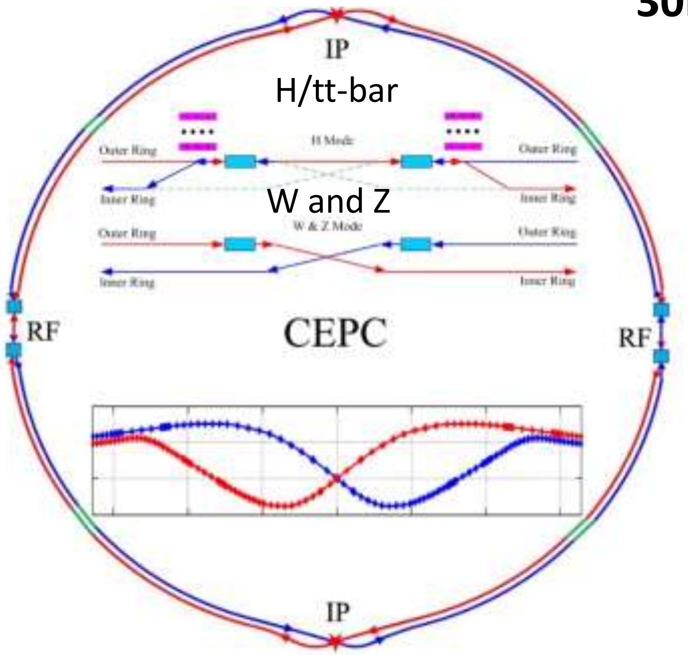

CEPC collider ring (100km)

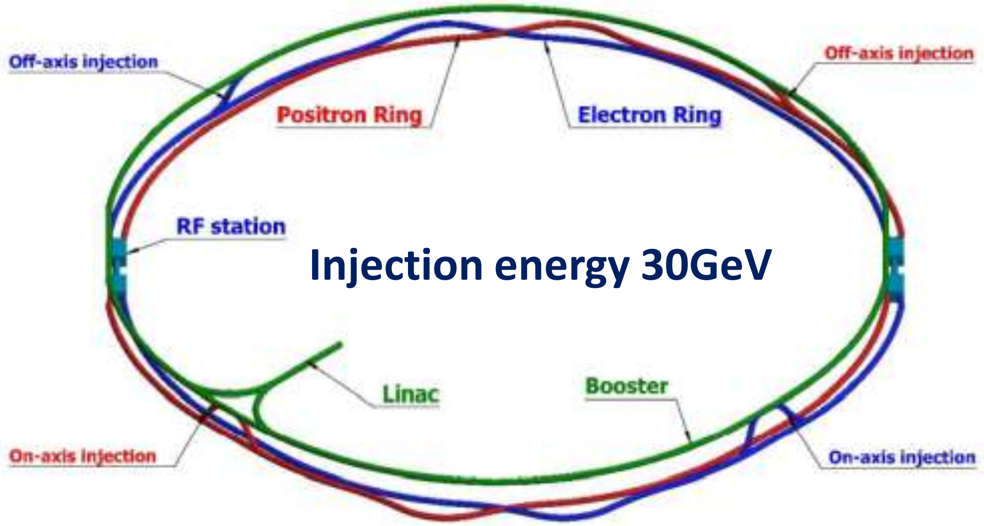

CEPC booster ring (100km)

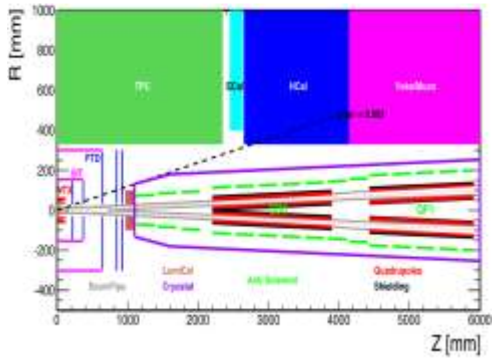

CEPC MDI

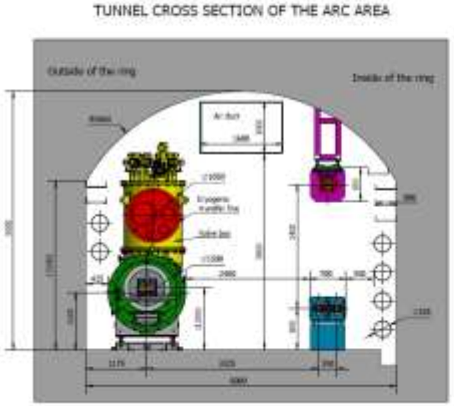

CEPC Civil Engineering

CEPC TDR S+C-band 30GeV linac injector

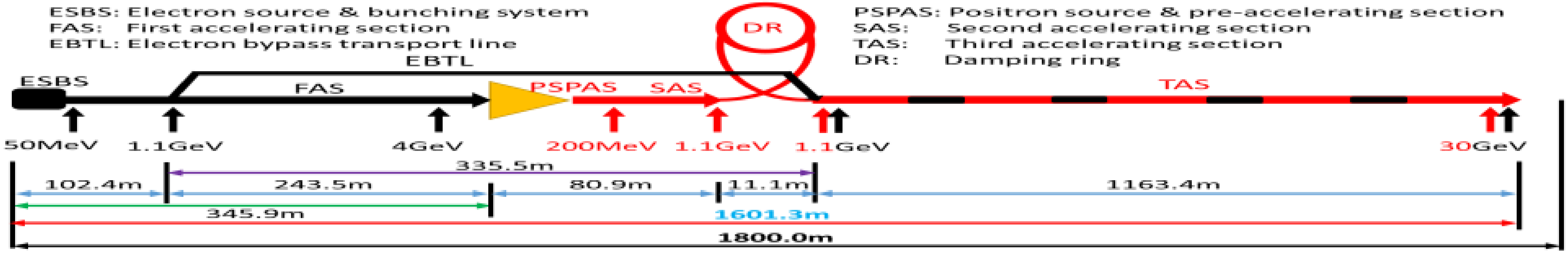

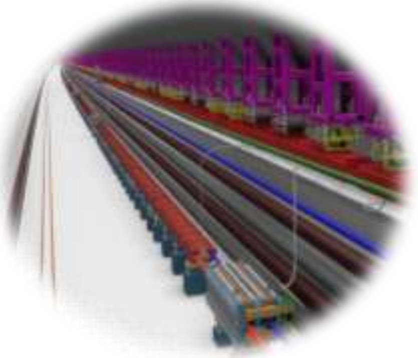

Lepton Circular Collider Design Procedure

Chinese Physics C Vol. 37, No. 9 (2013) 097003

Optimization parameter design of a circular e^+e^- Higgs factory*

WANG Dou(王逗)[1) GAO Jie(高杰) XIAO Ming(肖铭) GENG Hui-Ping(耿会平)
GUO Yuan-Yuan(郭媛媛) XU Shou-Yan(许守彦) WANG Na(王娜) AN Yu-Wen(安宇文)
QIN Qing(秦庆) XU Gang(徐刚) WANG Sheng(王生)
Institute of High Energy Physics (IHEP), Beijing 100049, China

Abstract: In this paper we will show a general method of how to make an optimized parameter design of a circular e^+e^- Higgs factory by using analytical expression of maximum beam-beam parameter and beamstrahlung beam lifetime starting from a given design goal and technical limitations. A parameter space has been explored. Based on beam parameters scan and RF parameters scan, a set of optimized parameter designs for 50 km Circular Higgs Factory (CHF) with different RF frequency was proposed.

Key words: circular Higgs factory (CHF), parameter design, optimization, RF technology

PACS: 29.20.db **DOI:** 10.1088/1674-1137/37/9/097003

1 Introduction

With the discovery of a Higgs boson on the Large Hadron Collider (LHC) at the energy of about 125 GeV [1, 2], the world high-energy physics community is investigating the feasibility of a Higgs factory, a complement to the LHC for studying the Higgs. The low Higgs mass makes a circular Higgs factory possible. Compared with the linear collider, the circular collier as a Higgs factory has mature technology and rich experience. Also, a circular Higgs factory has potentially a higher luminosity to cost ratio than a linear one at 240 GeV [3]. So, much attention is given to the design of a circular Higgs Factory and several proposals have recently been put forward [4–8]. In order to find the optimized machine parameter design starting from the required luminosity goal, beam energy, physical constraints at IP and some technical limitations, we study a general analytical method for the parameter choice based on the maximum beam-beam tune shift, beamstrahlung-driven lifetime and beamstrahlung energy spread.

low statistic laws. Apparently, the synchrotron radiation is the main source of heating. Besides, when two bunches undergo collision at an interaction point (IP), every particle in each bunch will feel the deflected electromagnetic field of the opposite bunch and the particles will suffer from additional heating. With the increase of the bunch particle population N_e, this kind of heating effect will get stronger and the beam emittance will increase. There is a limit condition beyond which the beam emittance will blow up. This emittance blow-up mechanism introduces a limit for beam-beam tune shift [9]

$$\xi_y \leqslant \frac{2845}{2\pi}\sqrt{\frac{T_0}{\tau_y \gamma N_{IP}}}, \qquad (1)$$

where N_{IP} is the number of interaction points (when there are N_{IP} interaction points, the independent heating effects have to be added in a statistical way), τ_y is the transverse damping time and T_0 is the revolution time.

3 Beam lifetime limit and energy spread limit due to beamstrahlung

Started from energy and maximum luminosity design goals, by using the analytical maximum beam-beam tune shift formulae, to derive all other beam and machine parameters Just like linear collider design introduced previously.

D. Wang, J. Gao, et al., “Optimization parameter design of a circular e+e- Higgs factory”, Chinese Physics C Vol. 37, No. 9 (2013) 097003.

To design crab-waist collision collider, just use the Corresponding beam-beam formular in this lecture shown previously on page 35.

CEPC TDR Parameters (30MW and 50MW SR/beam)

Table 4.1.1: CEPC baseline parameters in TDR

	Higgs	Z	W	$t\bar{t}$
Number of IPs	2			
Circumference (km)	100.0			
SR power per beam (MW)	30			
Half crossing angle at IP (mrad)	16.5			
Bending radius (km)	10.7			
Energy (GeV)	120	45.5	80	180
Energy loss per turn (GeV)	1.8	0.037	0.357	9.1
Damping time $\tau_x/\tau_y/\tau_z$ (ms)	44.6/44.6/22.3	816/816/408	150/150/75	13.2/13.2/6.6
Piwinski angle	4.88	24.23	5.98	1.23
Bunch number	268	11934	1297	35
Bunch spacing (ns)	591 (53% gap)	23 (18% gap)	257	4524 (53% gap)
Bunch population (10^{11})	1.3	1.4	1.35	2.0
Beam current (mA)	16.7	803.5	84.1	3.3
Phase advance of arc FODO (°)	90	60	60	90
Momentum compaction (10^{-5})	0.71	1.43	1.43	0.71
Beta functions at IP β_x^*/β_y^* (m/mm)	0.3/1	0.13/0.9	0.21/1	1.04/2.7
Emittance $\varepsilon_x/\varepsilon_y$ (nm/pm)	0.64/1.3	0.27/1.4	0.87/1.7	1.4/4.7
Betatron tune ν_x/ν_y	445/445	317/317	317/317	445/445
Beam size at IP σ_x/σ_y (um/nm)	14/36	6/35	13/42	39/113
Bunch length (natural/total) (mm)	2.3/4.1	2.5/8.7	2.5/4.9	2.2/2.9
Energy spread (natural/total) (%)	0.10/0.17	0.04/0.13	0.07/0.14	0.15/0.20
Energy acceptance (DA/RF) (%)	1.6/2.2	1.0/1.7	1.05/2.5	2.0/2.6
Beam-beam parameters ξ_x/ξ_y	0.015/0.11	0.004/0.127	0.012/0.113	0.071/0.1
RF voltage (GV)	2.2	0.12	0.7	10
RF frequency (MHz)	650			
Longitudinal tune ν_s	0.049	0.035	0.062	0.078
Beam lifetime (Bhabha/beamstrahlung) (min)	40/40	90/2800	60/195	81/23
Beam lifetime requirement (min)	18	77	22	18
Hourglass Factor	0.9	0.97	0.9	0.89
Luminosity per IP (10^{34} cm^{-2} s^{-1})	5.0	115	16	0.5
Luminosity per IP (10^34 cm^-2s^-1) from formula	**5**	**115**	**12**	**0.59**

Luminosity results calculated from eqs. A, B, C, D on previous page 35

Table 4.1.2: CEPC main parameters with 50 MW upgrade

	Higgs	Z	W	$t\bar{t}$
Number of IPs	2			
Circumference (km)	100.0			
SR power per beam (MW)	50			
Half crossing angle at IP (mrad)	16.5			
Bending radius (km)	10.7			
Energy (GeV)	120	45.5	80	180
Energy loss per turn (GeV)	1.8	0.037	0.357	9.1
Damping time $\tau_x/\tau_y/\tau_z$ (ms)	44.6/44.6/22.3	816/816/408	150/150/75	13.2/13.2/6.6
Piwinski angle	4.88	29.52	5.98	1.23
Bunch number	446	13104	2162	58
Bunch spacing (ns)	355 (53% gap)	23 (10% gap)	154	2714 (53% gap)
Bunch population (10^{11})	1.3	2.14	1.35	2.0
Beam current (mA)	27.8	1340.9	140.2	5.5
Phase advance of arc FODO (°)	90	60	60	90
Momentum compaction (10^{-5})	0.71	1.43	1.43	0.71
Beta functions at IP β_x^*/β_y^* (m/mm)	0.3/1	0.13/0.9	0.21/1	1.04/2.7
Emittance $\varepsilon_x/\varepsilon_y$ (nm/pm)	0.64/1.3	0.27/1.4	0.87/1.7	1.4/4.7
Betatron tune ν_x/ν_y	445/445	317/317	317/317	445/445
Beam size at IP σ_x/σ_y (um/nm)	14/36	6/35	13/42	39/113
Bunch length (natural/total) (mm)	2.3/4.1	2.7/10.6	2.5/4.9	2.2/2.9
Energy spread (natural/total) (%)	0.10/0.17	0.04/0.15	0.07/0.14	0.15/0.20
Energy acceptance (DA/RF) (%)	1.6/2.2	1.0/1.5	1.05/2.5	2.0/2.6
Beam-beam parameters ξ_x/ξ_y	0.015/0.11	0.0045/0.13	0.012/0.113	0.071/0.1
RF voltage (GV)	2.2	0.1	0.7	10
RF frequency (MHz)	650			
Longitudinal tune ν_s	0.049	0.032	0.062	0.078
Beam lifetime (Bhabha/beamstrahlung) (min)	40/40	90/930	60/195	81/23
Beam lifetime requirement (min)	20	81	25	18
Hourglass Factor	0.9	0.97	0.9	0.89
Luminosity per IP (10^{34} cm^{-2} s^{-1})	8.3	192	26.7	0.8
Luminosity per IP (10^34 cm^-2s^-1) from formula	**8.4**	**192**	**21**	**0.97**

J. Gao, CEPC Technical Design Report: Accelerator. **Radiat Detect Technol Methods** (2024). https://doi.org/10.1007/s41605-024-00463-y

D. Wang, J. Gao, et al., "Optimization parameter design of a circular e+e- Higgs factory", Chinese Physics C Vol. 37, No. 9 (2013) 097003.

Studies of Beam-Beam Effects in CEPC

Results from J. Gao's formulae

- Luminosity simulations w/ZL

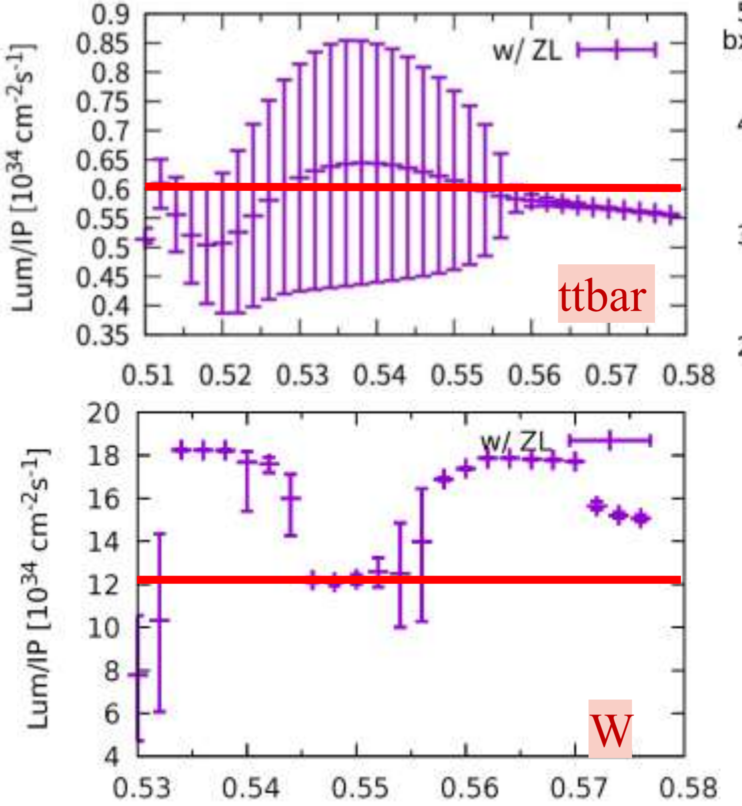

- Transverse size simulations

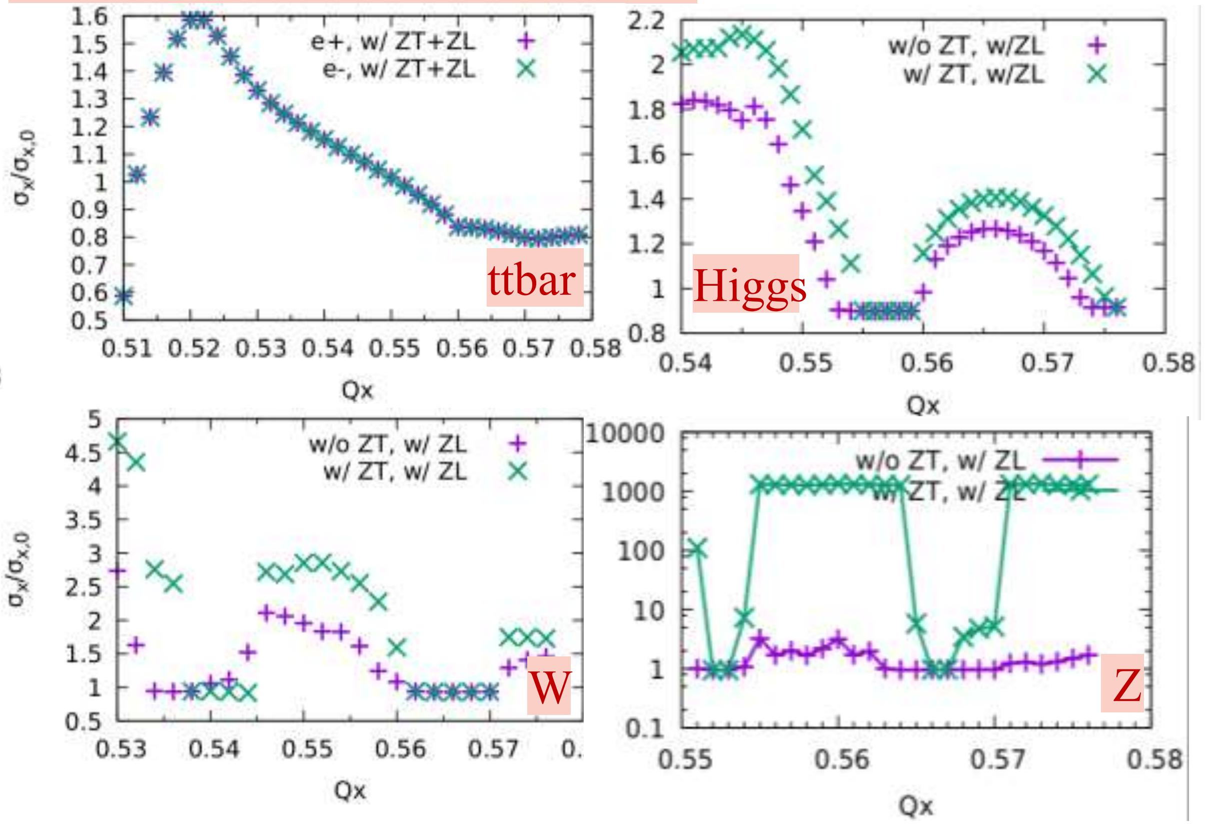

Above results from CEPC accelerator TDR: J. Gao, CEPC Technical Design Report: Accelerator. ***Radiat Detect Technol Methods (2024).*** https://doi.org/10.1007/s41605-024-00463-y

Beam-beam simulation results are consistent with the TDR parameter tables.

- Luminosity & Lifetime is evaluated by strong-strong simulation
- X-Z instability is well suppressed even considering Potential Well Distortion
- Lifetime optimization with both beam-beam\lattice nonlinearity is done

Hadron Circular Collider Design Procedure

Method Study of Parameter Choice for a Circular Proton-Proton Collider *

SU Feng[1] GAO Jie XIAO Ming WANG Dou
WANG Yi-Wei BAI Sha BIAN Tian-Jian

Key Laboratory of Particle Acceleration Physics and Technology, Institute of High Energy Physics,Chinese Academy of Sciences, Beijing 100049, China

Abstract: In this paper we showed a systematic method of appropriate parameter choice for a circular pp collider by using analytical expression of beam-beam tune shift limit started from given design goal and technical limitations. A parameter space has been explored. Based on parameters scan and considerations from RF systems, a set of appropriate parameter designed for a 50Km and a 100Km circular proton-proton collider was proposed.

Key words: circular proton-proton collider, parameter choice, beam-beam tune shift limit

PACS: 29.20.db

Feng Su (苏峰), Jie Gao (高杰), Ming Xiao (肖铭), Dou Wang (王逗), Yi-Wei Wang (王毅伟), Sha Bai (白莎) and Tian-Jian Bian (边天剑), “Method study of parameter choice for a circular proton–proton collider”, Chinese Physics C, Volume 40, Number 1 Citation Feng Su et al 2016 Chinese Phys. C 40 017001 DOI 10.1088/1674-1137/40/1/017001

Started from design energy and maximum Luminosity goal by using the analytical Maximum beam-beam tune shift formulae, to derive all other beam and machine parameters Just like linear collider and lepton circular Collider design introduced previously.

The maximum beam-beam tune shit formulae of hadron machine in the paper should be replaced by the maximum beam-beam tune shit formulae of round beam collision shown in this lecture shown previously.

SppC Collider TDR Parameters

Table 8.2.1: Main parameters of the SPPC

Parameter	Value	Unit
General design parameters		
Circumference	100	km
Beam energy	62.5	TeV
Lorentz gamma	66631	
Dipole field	20.3	T
Dipole curvature radius	10258.3	m
Arc filling factor	0.79	
Total dipole magnet length	64.455	km
Arc length	81.8	km
Number of long straight sections	8	
Total straight section length	18.2	km
Energy gain factor in collider rings	19.53	
Injection energy	3.2	TeV
Number of IPs	2	
Revolution frequency	3.00	kHz
Physics performance and beam parameters		
Initial luminosity per IP	4.3×10^{34}	$cm^{-2}s^{-1}$
Beta function at collision	0.50	m
Circulating beam current	0.19	A
Nominal beam-beam tune shift limit per IP	0.015	
Beam-beam tune shift calculated from Eqs. I or II	**0.0147**	
Bunch separation	25	ns
Number of bunches	10082	
Bunch population	4.0×10^{10}	
Accumulated particles per beam	4.0×10^{14}	
Normalized rms transverse emittance	1.2	μm
Beam lifetime due to burn-off	8.1	hours
Total inelastic cross section	161	mb
Reduction factor in luminosity	0.81	
Full crossing angle	73	μrad
rms bunch length	60	mm
rms IP spot size	3.0	μm
Beta at the first parasitic encounter	28.6	m
rms spot size at the first parasitic encounter	22.7	μm
Stored energy per beam	4.0	GJ
SR power per beam	2.2	MW
SR heat load at arc per aperture	27.4	W/m
Energy loss per turn	11.6	MeV

J. Gao, CEPC Technical Design Report: Accelerator. **Radiat Detect Technol Methods** (2024). https://doi.org/10.1007/s41605-024-00463-y

Beam-beam tune shift result calculated from Eqs. I or II of J. Gao on previous page 34

F. Su, J. Gao, et al., Method Study of Parameter Choice for a Circular Proton-Proton Collider, Chinese Physics C(2016), Vol. 40, Issue(1) : 017001 DOI: 10.1088/1674-1137/40/1/017001

Analytical wake potential of a storage ring

We start with finding an analytical expression that describes the wake potential of a storage ring. For the convenience of our theoretical treatment coming later, we will use a function of three parameters, i.e., bunch length σ_z, total loss factor $k(\sigma_z)$, and the total inductance $L(\sigma_z)$, to describe the total wake potential of the machine. As an Ansatz, we propose the following analytical expression:

$$\mathcal{W}_z(z) = -ak(\sigma_z)\exp\left(-\frac{2z^2}{7\sigma_z^2}\right)\times$$

$$\cos\left(\left(1+\frac{2}{\pi}\mathrm{atan}\left(\mathrm{atan}\left(\frac{Z_i}{2Z_r}\right)\right)\right)\frac{z}{\sqrt{3}\sigma_z}+\mathrm{atan}\left(\frac{Z_i}{2Z_r}\right)\right)$$

where $a = 2.23$, $Z_i = 2\pi L/T_0$, $Z_r = k(\sigma_z)\frac{T_b^2}{T_0}$, $T_0 = 2\pi R_{av}/c$, $T_b = 3\sigma_z/c$, R_{av} is the average radius of the ring, σ_z is the bunch length, c is the velocity of light, and $z = 0$ corresponds to the center of the bunch. The effectiveness of the wake potential expression

J. Gao, "On the single bunch longitudinal collective effects in electron storage rings", **Nucl. Instr. and Methods, A**491 2002, p.1

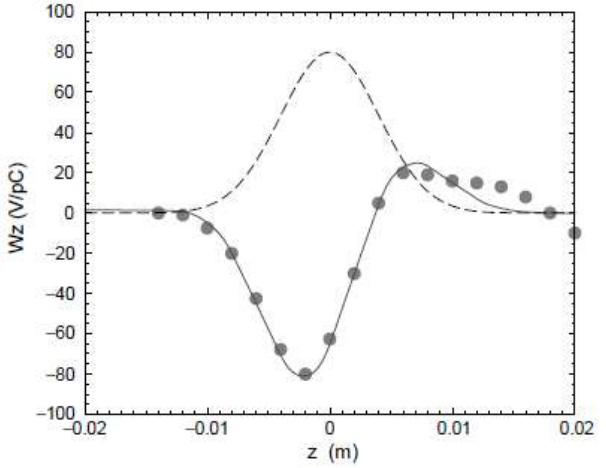

Fig. 1. KEKB low energy ring: the dots and the solid line represent the wake potentials calculated numerically [27] and analytically by using Eq. (2), respectively, with $\sigma_{z0} = 0.004$ m, $L = 22$ nH, and $k(\sigma_{z0}) = 42$ V/pC. The dashed line shows the Gaussian bunch shape with arbitrary units.

KEK B low energy ring wake potential

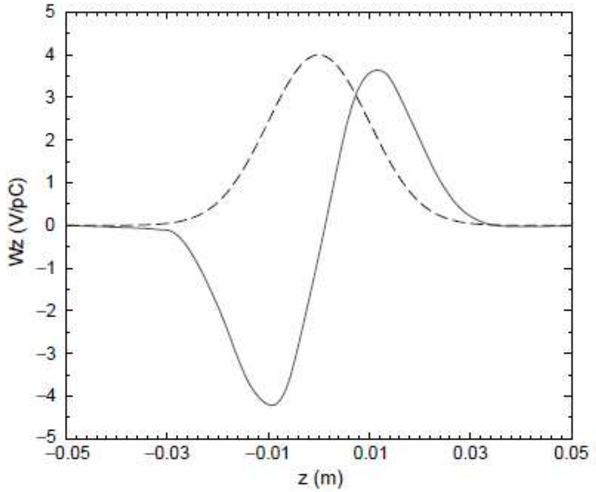

Fig. 3. The solid line represents the total longitudinal wake potential of PEP-II low energy ring with $\sigma_{z0} = 0.01$ m, $L = 83.3$ nH, and $k(\sigma_{z0}) = 2.9$ V/pC. The dashed line shows the Gaussian bunch shape with arbitrary units.

PEP-II low energy ring wake potential

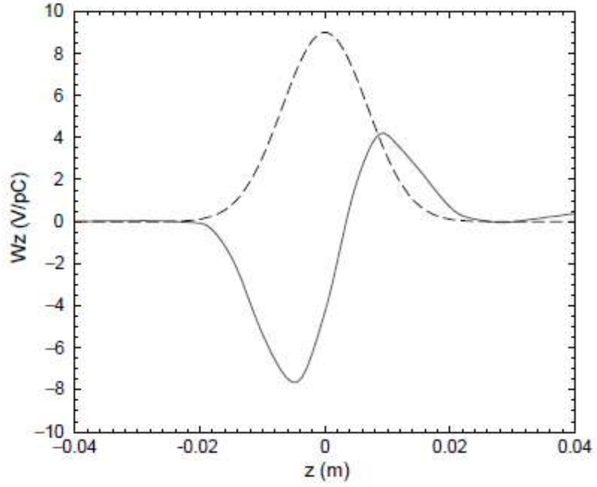

Fig. 5. The solid line corresponds to the total longitudinal wake potential of ATF damping ring with $\sigma_{z0} = 0.0068$ m, $L = 14$ nH, and $k(\sigma_{z0}) = 4.5$ V/pC. The dashed line shows the Gaussian bunch shape with arbitrary units.

KEK ATF storage ring wake potential

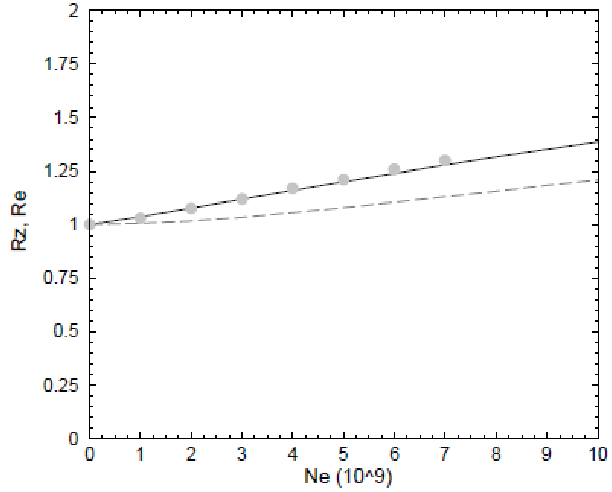

Fig. 6. ATF damping ring: the solid line and the dashed line are the bunch lengthening and the energy spread increasing vs. the particle population inside the bunch, respectively ($\sigma_{z0} = 0.0068$ m). The dots are experimental results.

Bunch lengthening and energy spread increasing in a storage ring

$$R_z^2 = 1 + \frac{C_{\mathrm{PWD}} I_b}{R_z^{1.5}} + \frac{\mathscr{C}(R_{\mathrm{av}} R I_b \mathscr{K}_{\|.0}^{\mathrm{tot}})^2}{\gamma^7 R_z^{2.42}} \qquad R_z = \sigma_z / \sigma_{z_0}$$

and Eq. (15)($\iota = \varepsilon$) remains

$$R_\varepsilon^2 = 1 + \frac{\mathscr{C}(R_{\mathrm{av}} R I_b \mathscr{K}_{\|.0}^{\mathrm{tot}})^2}{\gamma^7 R_z^{2.42}}. \qquad R_\varepsilon = \sigma_\varepsilon / \sigma_{\varepsilon_0}.$$

What should be pointed out is that $\mathscr{C}$ is a positive number, however, C_{PWD} can be negative if the momentum compaction factor, α, is negative. The procedure to get the information about the bunch lengthening and the energy spread increasing is firstly to solve Eq. (17) and find $R_z(I_b)$, and then calculate $R_\varepsilon(I_b)$ by putting $R_z(I_b)$ into Eq. (18). When the bunch current is high enough to neglect the effect of PWD, one has $R_\varepsilon \approx R_z$ which means that energy spread increasing and bunch lengthening are almost correlated. We point out that the third term in Eq. (17) might correspond to the so-called turbulent bunch lengthening observed in the experiments.

J. Gao, Bunch lengthening and energy spread increasing in electron
storage rings, **Nucl. Instr. and Meth. in Phys. Res. A** 418 (1998) 332—336

J. Gao, An empirical equation for bunch lengthening in electron storage rings, **Nuclear Instruments and Methods in Physics Research A** 432 (1999) 539}543

J. Gao, "On the single bunch longitudinal collective effects in electron storage rings", **Nucl. Instr. and Methods, A**491 2002, p.1

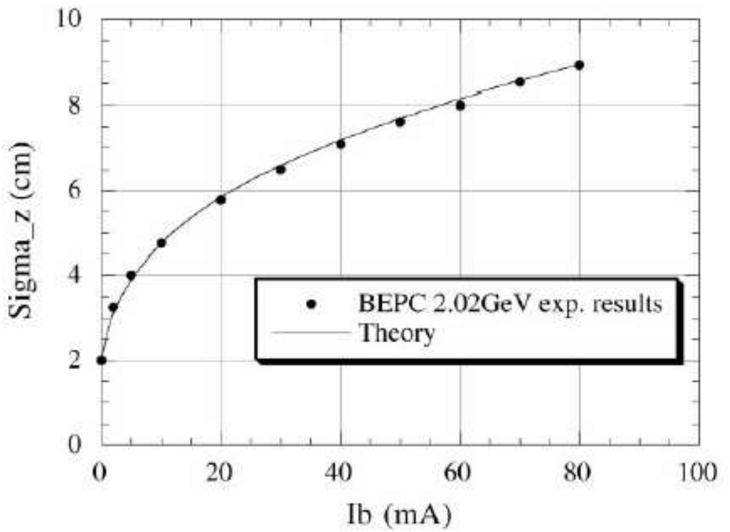

Fig. 1. Comparison between BEPC ($R = 10.345$ m and $R_{\mathrm{av}} = 38.2$ m) experimental results and the theoretical results at 2.02 GeV with $\sigma_{z_0} = 2$ cm. The continuous line is the fitted curve of the theory. The dark points are the BEPC 2.02 GeV experimental results.

Theory of single bunch transverse emittance growth in electron storage rings-1

Modern Physics Letters A
Vol. 30, No. 11 (2015) 1530006 (20 pages)

DOI: 10.1142/S0217732315300062

World Scientific
www.worldscientific.com

Review of some important beam physics issues in electron–positron collider designs

Jie Gao
Institute of High Energy Physics, Yuquan Road 19, Beijing 100049, P. R. China
gaoj@ihep.ac.cn

Received 11 December 2014
Accepted 15 January 2015
Published 25 March 2015

In this paper, we will give a brief review of some important beam physics in circular and linear electron–positron collider designs, covering beam–beam tune limits, longitudinal and transverse single bunch collective effects, electron cloud and space charge effects, dynamic aperture estimations, etc. The main feature of this review is that the corresponding beam physics treatments are coming from author's previous research works which are scattered in different scientific publications both for circular and linear colliders. With the progresses of future linear colliders, such as ILC,[1] and future circular electron–positron colliders, such as CEPC,[2] it is high time to review the key beam physics issues in the optimization designs of these two kinds of machines.

Keywords: Circular colliders; linear colliders; electron–positron; ILC; CEPC.

PACS Nos.: 29.20.db, 29.20.Dh, 29.20.Ej, 29.27.Bd

If we distinguish now the horizontal plane denoted by the subscript x and the vertical plane denoted by the subscript y, one gets two emittance equations

$$\mathcal{R}_{\epsilon,x} = \frac{\epsilon_{\mathrm{total},x}}{\epsilon_{0,x}} = 1 + \frac{\sigma_X^2 \tau_x \langle \beta_x(s) \rangle}{4T_0 \epsilon_{0,x} \mathcal{R}_{\epsilon,x}^3} \left(\frac{e^2 N_e k_{\perp,x}(\sigma_{z0})}{m_0 c^2 \gamma \mathcal{R}_z^{\Theta}} \right)^2 , \tag{34}$$

$$\mathcal{R}_{\epsilon,y} = \frac{\epsilon_{\mathrm{total},y}}{\epsilon_{0,y}} = 1 + \frac{\sigma_Y^2 \tau_y \langle \beta_y(s) \rangle}{4T_0 \epsilon_{0,y} \mathcal{R}_{\epsilon,y}^3} \left(\frac{e^2 N_e k_{\perp,y}(\sigma_{z0})}{m_0 c^2 \gamma \mathcal{R}_z^{\Theta}} \right)^2 , \tag{35}$$

where σ_{z0} is the bunch length of zero current, σ_X and σ_Y are standard deviations of the beam orbit with respect to the geometric center of vacuum chamber, $\langle \beta_x(s) \rangle$ and $\langle \beta_y(s) \rangle$ are the average of the beta functions over the ring, τ_x and τ_y are the damping times, $\epsilon_{0,x}$ and $\epsilon_{0,y}$ are the natural emittances, and T_0 is the revolution period, $\mathcal{R}_z = \sigma_z/\sigma_{z0}$, and $\Theta = 0.7$, which corresponds to SPEAR scaling for transverse loss factor.[28] Since $\mathcal{R}_z$ is also a function of N_e, it is obvious that one can start to solve Eqs. (34) and (35) only when $\mathcal{R}_z(N_e)$ has been solved from the bunch lengthening equation.[16] Equations (34) and (35) set the requirements on the orbit alignment tolerances with respect to the center of vacuum chamber.

Jie Gao, Review of some important beam physics issues in electron positron collider designs, **Modern Physics Letters A** Vol. 30, No. 11 (2015) 1530006 (20 pages) , DOI: 10.1142/S0217732315300062

Jie Gao, Analytical Treatment of Some Selected Problems in Particle Accelerators, LAL/RT 03-04, LAL, Orsay, France, p. 96-104

Theory of single bunch transverse emittance growth in electron storage rings-2

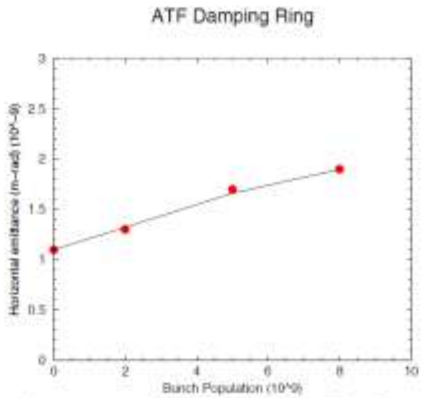

Figure 9.3: Horizontal emittance vs bunch population. The dots and solid line correspond to the experimental and theoretical values, respectively.

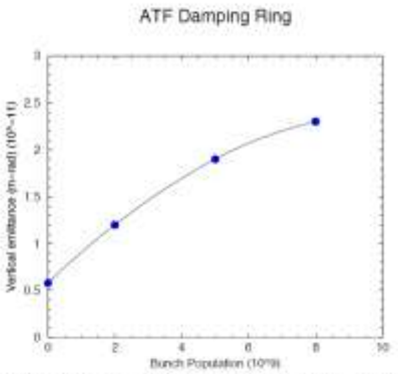

Figure 9.4: Vertical emittance vs bunch population. The dots and solid line correspond to the experimental and theoretical values, respectively.

9.4 Application to the analysis of ATF damping ring experimental results

ATF damping ring is a machine dedicated for the feasibility studies of future e^+e^- linear colliders [15]. In this section, by applying our theory established above and neglecting intrabeam scattering effects, we try to explain the ATF damping ring experimental results [6] with the following machine parameters: $E_0 = 1.3$ GeV, $<\beta_x> = 4.2$ m, $<\beta_y> = 4.6$ m, $\tau_x = 18.2$ ms, $\tau_y = 29.2$ ms, $\epsilon_{x0} = 1.1 \times 10^{-9}$ mrad, $\epsilon_{y0} = 5.8 \times 10^{-11}$ mrad, and the information about the bunch lengthening with respect to N_e can be obtained either from experimental results [10][11] or from analytical results [13] as shown in Fig. 9.2. Assuming $k_{\perp,x}(\sigma_{z0}) = k_{\perp,y}(\sigma_{z0})$=1020 V/pC/m, for $\sigma_X = 0.42$ mm and $\sigma_Y = 0.163$ mm, by using eqs. 9.23 and 9.24 one fits the experimentally measured emittance grow ups vs the bunch population as illustrated in Figs. 9.3 and 9.4, where the experimental results correspond to the values denoted in ref. [6] as "Wire scanner 2001/2/8". It is seen clearly that both the horizontal and vertical emittances' functional dependences on the bunch population fit well with the experimental results. We stress that $\sigma^2_{X,Y} = \sigma^2_{x,y,chamber} + \sigma^2_{x,y,co}$, where $\sigma_{x,y,chamber}$ are the vacuum chamber misalignment errors and $\sigma_{x,y,co}$ are the closed orbit distortion errors. It is obvious that to avoid excessive emittance grow ups, both the closed orbit distortions and the vacuum chamber misalignment errors should be under careful controlls with the same rigour.

101

Small emittances are vital for advanced light sources and high luminosity linear collider damping rings and circular colliders with carb-waist collisions

Jie Gao, Analytical Treatment of Some Selected Problems in Particle Accelerators, LAL/RT 03-04, LAL, Orsay, France, p. 96-104

Theory of single bunch transverse collective instabilities in electron storage rings

In an electron storage ring the maximum single-bunch current is usually limited by a fast transverse bunch size blow-up in the vertical plane when the single-bunch current passes an obvious threshold as was observed in PETRA [1] and the other machines. Nowadays, the theoretical explanation to this phenomenon is based on the so-called transverse mode coupling theory originally proposed by Kohaupt [1] and enriched by many others [2–4]. The well-accepted threshold current from the mode coupling theory reads

Kohaupt's formula

$$I_{\mathrm{b,coupling}}^{\mathrm{th}} = \frac{f_s E_0}{e\langle\beta_{y,c}\rangle \mathscr{K}_{\perp}^{\mathrm{tot}}(\sigma_z)}, \tag{1}$$

where f_s is the synchrotron oscillation frequency, E_0 is the particle energy, $\langle\beta_{y,c}\rangle$ is the average vertical beta function at RF cavities, and $\mathscr{K}_{\perp}^{\mathrm{tot}}(\sigma_z)$ is the total transverse loss factor at bunch length σ_z. The

B. Zotter's formula

$$I_{\mathrm{b,zotter}}^{\mathrm{th}} = \frac{F f_s E_0}{e\langle\beta_{y,c}\rangle \mathscr{K}_{\perp}^{\mathrm{tot}}(\sigma_z)} \tag{2}$$

J. Gao's formula

$$I_{\mathrm{b,gao}}^{\mathrm{th}} = \frac{F' f_s E_0}{e\langle\beta_{y,c}\rangle \mathscr{K}_{\perp}^{\mathrm{tot}}(\sigma_z)} \tag{12}$$

with

$$F' = 4R_z|\xi_{c,y}|\frac{\nu_y \sigma_{\varepsilon 0}}{\nu_s E_0}. \tag{13}$$

J. Gao, Theory of single bunch transverse collective instabilities in electron storage rings, **Nucl. Instr. and Meth. in Phys. Res. A** 416 (1998) 186-188

Below microwave instability

$$I_{\mathrm{th}} = \left(\frac{4 f_y \sigma_{\varepsilon 0} C^{\Theta} |\xi^*_{c,y}|}{e \langle \beta_{y,c} \rangle K_{\perp}^{\mathrm{tot}}(\sigma_{z0})} \right)^{3/(3-\Theta)}$$

and

Above microwave instability

$$I_{\mathrm{th}} = \left(\frac{4 f_y \sigma_{\varepsilon 0} C^{\Theta+1} |\xi^*_{c,y}|}{e \langle \beta_{y,c} \rangle K_{\perp}^{\mathrm{tot}}(\sigma_{z0})} \right)^{3/(2-\Theta)}.$$

$$\Theta = 0.7$$

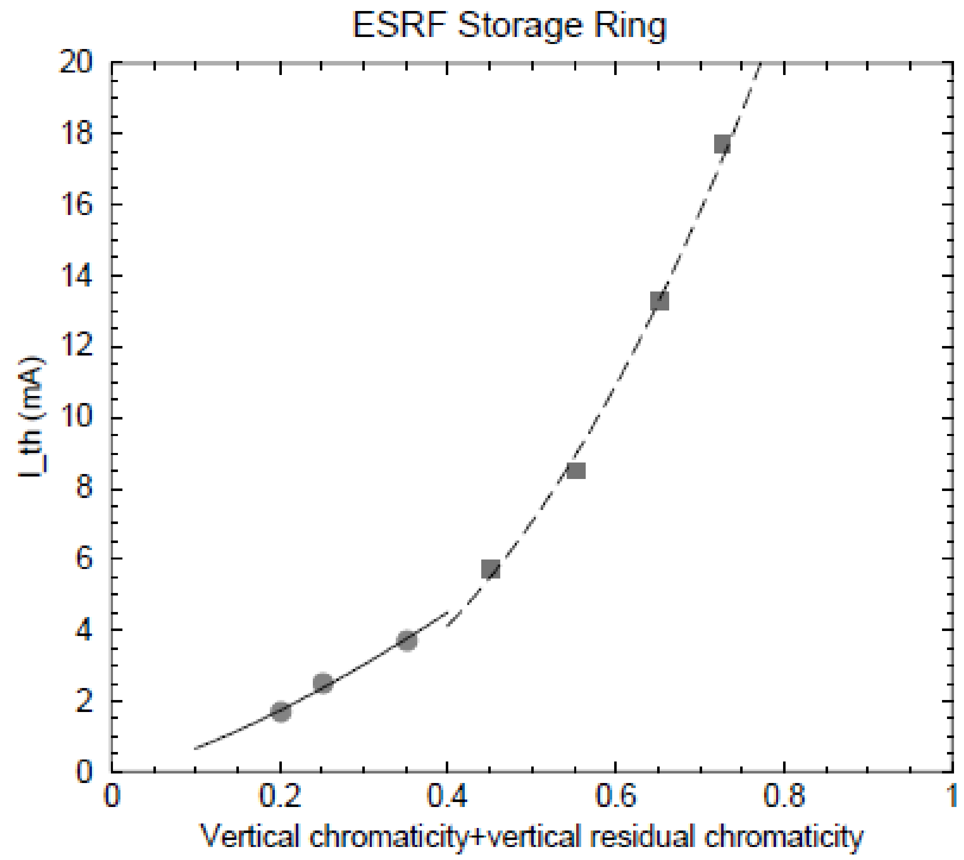

Fig. 2. The threshold bunch current vs. $\xi^*_{c,y}$ ($\xi_{c0,y} = 0.00211$): the dots and the squares represent the experimental results, and the solid and the dashed lines represent two fitting curves. The fitting formula is $y = ax^b$, and the fitting results are $a = 15.98$ (mA), $b = 1.38$ for solid line, and $a = 37.17$ (mA), $b = 2.39$ for dashed line, respectively.

J. Gao, On the scaling law of single bunch transverse instability threshold current vs. the chromaticity in electron storage rings, **Nuclear Instruments and Methods in Physics Research A** 491 (2002) 346–348

Summary

The fundamental beam physics in a storage ring are single particle effects, such as dynamic apertures, and collective effects, such as beam-beam effects in both lepton and hadron circular colliders, wake potential of a storage ring, single bunch longitudinal and transverse instabilities, etc.

The above mentioned problems could be treated in analytical ways, and the corresponding theories have been presented.

Some concrete applications have been given.

Theoretical understanding of the fundamental physics problems in storage rings and circular colliders are very important in machine designs and operations.

References

1) J. Gao, "Analytical estimation on the dynamic apertures of circular accelerators", **Nucl. Instr. and Methods, A**451 (2000), p. 545.

2) J. Gao, Analytical estimation of dynamic apertures limited by the wigglers in storage rings", **Nucl. Instr. and Methods, A**516 2004, p. 243.

3)J. Gao, Analytical estimation of the beam-beam interaction limited dynamic apertures and lifetimes in e+e¡ circular colliders", **Nucl. Instr. and Methods, A**463 (2001), p. 50.

4) J. Gao, Analytical estimation of the effects of crossing angle on the luminosity of an e+e- circular collider", **Nucl. Instr. and Methods, A**481 (2001), p. 756.

5) J. Gao, Emittance growth and beam lifetime limitations due to beam–beam effects in e+e- storage ring colliders, **Nuclear Instruments and Methods in Physics Research A** 533 (2004) 270–274

6) J. Gao, “Analytical treatment of the nonlinear electron cloud effect and the combined effects with beam-beam and charge nonlinear forces in storage rings”, **Chinese Physics C** Vol. 33, No. 2, Feb., 2009, 135-144

7)J. Gao, Theoretical analysis of the limitation from the nonlinear space charge forces to TESLA damping ring, **TESLA 2003-12**

8) J. Gao, "Bunch lengthening and energy spread increasing in electron storage rings", **Nucl. Instr. and Methods A**418 (1998), p. 332.

9)J. Gao, "An empirical equation for bunch lengthening in electron storage rings", **Nucl. Instr. and Methods A**432 (1999), p. 539.

10) J. Gao, "On the single bunch longitudinal collective effects in electron storage rings", **Nucl. Instr. and Methods, A**491 2002, p.1

References

11) J. Gao, "Theory of single bunch transverse collective instabilities in electron storage rings", **Nucl. Instr. and Methods, A**416 (1998), p.186.
12) J. Gao, "On the scaling law of the single bunch transverse instability threshold current vs the chromaticity in electron storage rings", **Nucl. Instr. and Methods, A**491 2002, p. 346.
13） J. Gao, Review of some important beam physics issues in electron positron collider designs, **Modern Physics Letters A** Vol. 30, No. 11 (2015) 1530006 (20 pages)
14) J. Gao, "Emittance Growth and Beam Lifetime due to Beam-Beam Interaction in a Circular Collider", **Personal note**, 2004 (LAL, Orsay)
15) J. Gao, et al, "Analytical estimation of maximum beam-beam tune shifts for electron-positron and hadron circular colliders", Proceedings of ICFA Workshop on High Luminosity Circular e+e- Colliders – Higgs Factory, 2014
16) J. Gao, Review of Different Colliders", **International Journal of Modern Physics A**, (2021) 2142002 (25 pages).
17) J. Gao, "CEPC: future circular electron postron collider", **AAPPS Bulletin**, 2020, AUGUST 2020 vol. 30 no. 4.
18) J. Gao, "CEPC and SppC Status" —From the completion of CDR towards TDR, **International Journal of Modern Physics A**, Vol. 36, No. 22, 2142005 (2021).
19) The CEPC Study Group, CEPC Conceptual Design Report, Volume I-Accelerator, IHEP-CEPC-DR-2018-01, IHEP-AC-2018-01, August 2018, ArXiv:1809.00285.http://cepc.ihep.ac.cn/CEPC_CDR_Vol1_Accelerator.pdf
20) CEPC Accelerator white paper to Snowmass21, CEPC Accelerator Group, J. Gao, **arXiv:**2203.09451
21) J. Gao, CEPC Technical Design Report: Accelerator. Radiat Detect Technol Methods (2024). https://doi.org/10.1007/s41605-024-00463-y.
22) Jie Gao, "Analytical Treatment of Some Selected Problems in Particle Accelerators", LAL/RT 03-04, LAL, Orsay, France
23) D. Wang, J. Gao, et al., "Optimization parameter design of a circular e+e- Higgs factory", Chinese Physics C Vol. 37, No. 9 (2013) 097003.
24) F. Su, J. Gao, et al., Method Study of Parameter Choice for a Circular Proton-Proton Collider, Chinese Physics C(2016), Vol. 40, Issue(1) : 017001 DOI: 10.1088/1674-1137/40/1/017001

Some references could be down loaded from following website:http://indico.ihep.ac.cn/event/7393/

Thanks